JVI Journals.ASM.org

Sp100 Isoform-Specific Regulation of Human Adenovirus 5 Gene Expression

Julia Berscheminski,[a] Peter Wimmer,[a] Juliane Brun,[a] Wing Hang Ip,[a] Peter Groitl,[a] Tim Horlacher,[a] Ellis Jaffray,[b] Ron T. Hay,[b] Thomas Dobner,[a] Sabrina Schreiner[a]

Heinrich Pette Institute, Leibniz Institute for Experimental Virology, Hamburg, Germany[a]; Wellcome Trust Centre for Gene Regulation and Expression, College of Life Sciences, University of Dundee, Dundee, United Kingdom[b]

ABSTRACT

Promyelocytic leukemia nuclear bodies (PML-NBs) are nuclear structures that accumulate intrinsic host factors to restrict viral infections. To ensure viral replication, these must be limited by expression of viral early regulatory proteins that functionally inhibit PML-NB-associated antiviral effects. To benefit from the activating capabilities of Sp100A and simultaneously limit repression by Sp100B, -C, and -HMG, adenoviruses (Ads) employ several features to selectively and individually target these isoforms. Ads induce relocalization of Sp100B, -C, and -HMG from PML-NBs prior to association with viral replication centers. In contrast, Sp100A is kept at the PML tracks that surround the newly formed viral replication centers as designated sites of active transcription. We concluded that the host restriction factors Sp100B, -C, and -HMG are potentially inactivated by active displacement from these sites, whereas Sp100A is retained to amplify Ad gene expression. Ad-dependent loss of Sp100 SUMOylation is another crucial part of the virus repertoire to counteract intrinsic immunity by circumventing Sp100 association with HP1, therefore limiting chromatin condensation. We provide evidence that Ad selectively counteracts antiviral responses and, at the same time, benefits from PML-NB-associated components which support viral gene expression by actively recruiting them to PML track-like structures. Our findings provide insights into novel strategies for manipulating transcriptional regulation to either inactivate or amplify viral gene expression.

IMPORTANCE

We describe an adenoviral evasion strategy that involves isoform-specific and active manipulation of the PML-associated restriction factor Sp100. Recently, we reported that the adenoviral transactivator E1A targets PML-II to efficiently activate viral transcription. In contrast, the PML-associated proteins Daxx and ATRX are inhibited by early viral factors. We show that this concept is more intricate and significant than originally believed, since adenoviruses apparently take advantage of specific PML-NB-associated proteins and simultaneously inhibit antiviral measures to maintain the viral infectious program. Specifically, we observed Ad-induced relocalization of the Sp100 isoforms B, C, and HMG from PML-NBs juxtaposed with viral replication centers. In contrast, Sp100A is retained at Ad-induced PML tracks that surround the newly formed viral replication centers, acting as designated sites of active transcription. The host restriction factors Sp100B, -C, and -HMG are potentially inactivated by active displacement from these sites, whereas Sp100A is retained to amplify Ad gene expression.

Sp100 (speckled protein of 100 kDa) is an interferon (IFN)-inducible acidic protein with both transcription-activating and -repressive properties (1–3). Initially, Sp100 was described as an autoantigen recognized by antibodies from patients suffering from primary biliary cirrhosis (4–6). Similar to the *pml* gene (7, 8), several alternatively spliced mRNAs are expressed from the human *sp100* gene (1, 2, 4, 6, 9–12). Humans are so far known to express four different Sp100 isoforms: Sp100A, Sp100B, Sp100C, and Sp100HMG. All of them share the same N terminus, with an HSR (homogenously stained region) domain for dimerization and localization to promyelocytic leukemia nuclear bodies (PML-NBs) (13). Only Sp100B, -C, and -HMG contain a SAND (Sp100, AIRE-1, NucP41/45, and DEAF-1) domain exhibiting high affinity for DNA with unmethylated CpGs (14, 15).

Sp100C and Sp100HMG contain additional domains, such as a bromodomain, a plant homeodomain (PHD), and a high-mobility-group (HMG) domain (see Fig. 2A) (11). All of these domains have previously been shown to mediate association with chromatin (3, 16–19). Recently, Newhart and coworkers proposed the model that Sp100A increases chromatin decondensation, whereas the SAND domain in isoforms Sp100B, -C, and -HMG promotes chromatin condensation, suggesting that these proteins play a different role in transcriptional regulation (20).

All Sp100 isoforms are posttranslationally modified by small ubiquitin-related modifier (SUMO) proteins (21). However, in contrast to the case for PML, which requires SUMO modification for the formation of mature PML-NBs (22), SUMO modification of Sp100 is apparently not a prerequisite for nuclear body targeting. More likely, SUMO modification of Sp100 regulates its interaction with HP1 (heterochromatin protein 1) and other nonhistone chromosomal proteins (11, 18), forming a chromatin-associated complex and likely repressing gene expression (3, 18).

Received 14 February 2014 **Accepted** 10 March 2014
Published ahead of print 12 March 2014
Editor: M. J. Imperiale
Address correspondence to Thomas Dobner, thomas.dobner@hpi.uni-hamburg.de.
Copyright © 2014, American Society for Microbiology. All Rights Reserved.
doi:10.1128/JVI.00469-14

PML-NBs initially appeared to be involved in the pathogenesis of certain human diseases (7, 23–34) and were later found to be induced by interferon, upon viral infection, to exert their antiviral properties (35–38). The PML protein itself and Sp100 seem to be responsible for the assembly of nuclear bodies by recruiting other constitutive components, such as Daxx (death domain-associated protein) and SUMO (small ubiquitin-related modifier) (39–41).

Since they are critical for the formation and stability of these nuclear subdomains (39, 42–44), SUMOylated proteins are associated with PML-NBs at a high density (40, 45). Intriguingly, SUMO1 is detected mainly in the protein shell formed by PML and Sp100, whereas SUMO2/3 chains are also found in the interior of the PML-NB, mediating interactions with proteins transiently localizing to these domains (46). Since SUMO proteins regulate many different processes within the cell (45, 47), it is not surprising that viral pathogens take advantage of this posttranslational modification (PTM) to manipulate cellular pathways and maintain the integrity of viral proteins (48–50).

PML-NBs have been implicated in a general antiviral capacity based on recruitment of host restriction factors. This idea is supported by initial observations that PML and PML-associated proteins are encoded by interferon-stimulated genes, and thus also capable of impairing virus replication. This assumption appears reasonable, as many viruses encode early regulatory proteins that counteract PML-mediated antiviral activities (51). However, growing evidence points to the molecular mechanisms involved being more complicated.

We recently reported that the adenovirus (Ad) transactivator protein E1A targets the PML-II isoform to efficiently activate viral and cellular transcription (52). In contrast, the PML-associated proteins Daxx and ATRX, involved in cellular chromatin remodeling processes, are inhibited by either E1B-55K alone or in combination with the E4orf6 early viral factor (2–4, 53). This implies that viral proteins specifically target and counteract repressive proteins in PML bodies and take advantage of other PML-associated factors to promote efficient viral gene expression.

Here we demonstrate Ad-induced relocalization of the alternatively spliced Sp100 isoforms B, C, and HMG from PML-NBs prior to their association with viral replication centers. In contrast, isoform Sp100A is retained at the PML track-like structures surrounding the newly formed viral replication centers, which represent designated sites of active transcription. The host restriction factors Sp100B, -C, and -HMG are potentially inactivated by active displacement from these sites, whereas Sp100A remains to amplify Ad gene expression.

MATERIALS AND METHODS

Cell culture. HepaRG (54), HepaRG shSp100 (55), H1299 (56), and U2OS shDaxx (57) cells and HeLa cells stably expressing 6His-SUMO-1 and -2 (53) were grown in Dulbecco's modified Eagle's medium (DMEM) supplemented with 10% fetal calf serum (FCS), 100 U of penicillin per ml, and 100 μg of streptomycin per ml in a 5% CO_2 atmosphere at 37°C. For HepaRG cells, the medium was additionally supplemented with 5 μg/ml of bovine insulin and 0.5 μM hydrocortisone. U2OS shDaxx and HeLa 6His-SUMO cell lines were maintained under 2 μM puromycin selection. shSp100 cells were transduced with lentivirus vectors expressing short hairpin RNA (shRNA) as described by Everett et al. (55). The sense-strand DNA sequence of the anti-Sp100 shRNA was 5′-GTGAGCCTGTGATCA ATAA-3′, which corresponds to a sequence common to all Sp100 isoforms.

Plasmids and transient transfections. For transfections, we generated an N-terminally Flag-tagged human Sp100C isoform and used recently described A, B, and HMG constructs (58), yellow fluorescent protein (YFP)-tagged HP1α, YFP-tagged HP1β, human p53 (52), E2F-1 (52), and pG4–p300 (52). The Sp100A-SIM, E1A-13S–D121A, and E1A-12S–D121A mutations were introduced by site-directed mutagenesis using the following oligonucleotides: for Sp100A-SIM, forward primer 5′-CAGGC ATCTGACAAAAAAGTCATCAGCAG-3′ and reverse primer 5′-CTGCT GATGACTTTTTTGTCAGATGCCTG-3′; and for E1A-13S–D121A and E1A-12S–D121A, forward primer 5′-GGAGGTGATCGCTCTTACCTG C-3′ and reverse primer 5′-GCAGGTAAGAGCGATCACCTCC-3′. For transient transfection, subconfluent cells were treated with a mixture of DNA and 25-kDa linear polyethylenimine (Polysciences) as described previously (59). HeLa cells were transfected using Fugene 6 (Roche) according to the manufacturer's instructions.

Viruses. H5*pg*4100 served as the wild-type (wt) virus (60). H5*pm*4150 carries a frameshift mutation in the E4orf3 open reading frame, and H5*pm*4149 and H5*pm*4154 carry stop codons in the E1B-55K and E4orf6 open reading frames, to prevent expression of E4orf3, E1B-55K, and E4orf6, respectively (61, 62). All viruses were propagated and titrated as described previously (60). To measure virus growth, infected cells were harvested at 48 h postinfection (p.i.) and lysed by three cycles of freeze-thawing. The cell lysates were serially diluted in DMEM for infection of HEK293 cells, and virus yields were determined by quantitative E2A immunofluorescence staining at 24 h p.i.

Luciferase reporter assay. For dual-luciferase assays, subconfluent cells were transfected as described above, using 0.5 to 1 μg of reporter (pGL-E1A-promoter, pGL-E2early-promoter, pGL-E3-promoter, or pGL-pIX-promoter), 1 μg of pRL-TK (Promega), which expresses *Renilla* luciferase under the control of the herpes simplex virus thymidine kinase (HSV-TK) promoter, and 0.5 to 1 μg of effector plasmids (for Sp100A, Sp100B, Sp100C, and Sp100HMG). Cell extracts were prepared, measured, and normalized as described recently (63). For green fluorescent protein (GFP) control measurement (pEGFP-C1; Clontech), the medium was replaced with phosphate-buffered saline (PBS; 300 μl/well) at 24 h posttransfection, and the GFP fluorescence signal was measured using a Tecan Infinite 200 Pro plate reader in bottom-reading mode according to the manufacturer's protocol (excitation wavelength, 483 nm; excitation bandwidth, 9 nm; emission wavelength, 535 nm; emission bandwidth, 20 nm; gain, optimal; and integration time, 20 μs) before performing the luciferase reporter assay.

Antibodies and protein analysis. Primary antibodies specific for Ad proteins included E1A mouse monoclonal antibody (MAb) M58 (kindly provided by R. Grand), E2A mouse MAb B6-8 (64), rabbit polyclonal antibody (pAb) anti-E2A (kindly provided by R. T. Hay), E1B-55K mouse MAb 2A6 (65), E4orf6 mouse MAb RSA3 (66), E4orf3 rat MAb 6A11 (67), and Ad rabbit polyclonal serum L133 (68). Primary antibodies specific for cellular and ectopically expressed proteins included PML rabbit pAb NB100-59787 (Novus Biologicals, Inc.), Sp100 rabbit pAb GH3 (kindly provided by H. Will), mouse MAb Flag-M2 (Sigma-Aldrich, Inc.), β-actin mouse MAb AC-15 (Sigma-Aldrich, Inc.), a 6His mouse MAb (Clontech), and a GFP epitope MAb (Abcam). All protein extracts were prepared in RIPA lysis buffer as described recently (69). For immunoprecipitation of YFP-tagged HP1, a GFP-Trap kit (Chromotek) was used according to the manufacturer's protocol. Precipitated proteins were boiled for 3 min at 95°C in 2× Laemmli buffer and analyzed by immunoblotting exactly as described recently (59).

Indirect immunofluorescence assay. For indirect immunofluorescence assay, cells were grown on glass coverslips as already published (70). Cells were fixed in 4% paraformaldehyde (PFA) at 4°C for 20 min and permeabilized in PBS with 0.5% Triton X-100 for 30 min at room temperature. After 1 h of blocking in Tris-buffered saline–BG (TBS-BG; BG is 5% [wt/vol] BSA and 5% [wt/vol] glycine) buffer, coverslips were treated for 1 h with the primary antibody diluted in PBS, washed three times in PBS with 0.1% Tween 20, and then incubated with the corresponding

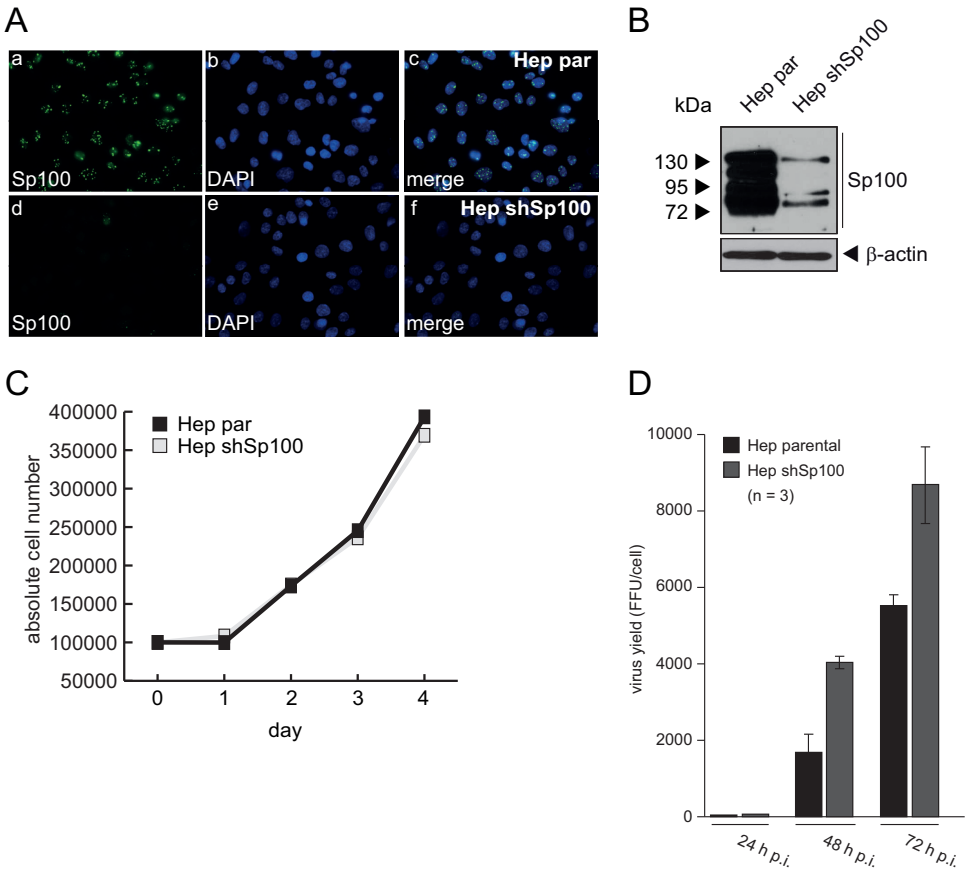

FIG 1 Sp100 depletion promotes Ad progeny production. (A) HepaRG parental (Hep par) and shSp100 (Hep shSp100) cells were fixed with 4% PFA, labeled with pAb GH3 (anti-Sp100), and detected with Alexa 488-conjugated secondary Ab (anti-Sp100; green). Nuclei were labeled with DAPI (4′,6-diamidino-2-phenylindole). Representative anti-Sp100 (green; panels a and d) and DAPI (blue; panels b and e) staining patterns and overlays of the single images (merge; panels c and f) are shown. Magnification, ×7,600. (B) Total cell extracts of parental and shSp100 HepaRG cells were prepared, and proteins were separated by SDS-PAGE and subjected to immunoblotting using pAb GH3 (anti-Sp100) and a mouse MAb (anti-AC-15). (C) Total cell numbers of parental and shSp100 HepaRG cells were determined at the indicated time points. (D) HepaRG parental (Hep par) and shSp100 (Hep shSp100) cells were infected with wt virus H5*pg*4100 at a multiplicity of infection of 50 focus-forming units (FFU)/cell. Viral particles were harvested at 24, 48, and 72 h p.i., and virus yields were determined by quantitative E2A-72K immunofluorescence staining.

Alexa 488 (Invitrogen)- or Cy3 (Dianova)-conjugated secondary antibody. Coverslips were washed three times in PBS with 0.1% Tween 20 and mounted in Glow medium (Energene), and digital images were acquired with a confocal laser scanning microscope (CLSM-510; Zeiss). Images were cropped using Adobe Photoshop CS4 and assembled with Adobe Illustrator CS6.

***In situ* hybridization.** Cy3-labeled fiber-specific oligonucleotides were generated with a Cy3 monoreactive dye pack (Amersham Biosciences) according to the manufacturer's recommendations. For *in situ* hybridization, cells were grown on glass coverslips, washed with PBS, and fixed for 15 min with 4% formaldehyde and 10% acetic acid. After washing steps with PBS, cells were permeabilized overnight at 4°C with 70% ethanol. Cells were then rehydrated for 5 min at room temperature with 2× SSC (1× SSC is 0.15 M NaCl plus 0.015 M sodium citrate) plus 50% formamide prior to labeling with the probes (30 ng). Hybridization was performed overnight at 37°C, with samples protected from light. Probes were washed twice for 1 h at 37°C with a 2× SSC–50% formamide–0.1% NP-40 solution. For the costaining of adenovirus replication centers (E2A), we performed an indirect immunofluorescence assay as described above. Hybridization was visualized with a confocal laser scanning microscope (CLSM-510; Zeiss). Images were cropped using Adobe Photoshop CS4 and assembled with Adobe Illustrator CS6.

Denaturing purification and analysis of SUMO conjugates. HeLa cells were infected or transfected with the appropriate expression vector. Forty-eight hours later, cells were lysed in 5 ml of 6 M guanidinium-HCl, 0.1 M Na_2HPO_4, 0.1 M NaH_2PO_4, 10 mM Tris-HCl, pH 8.0, 20 mM imidazole, and 5 mM β-mercaptoethanol (71). Ten percent of the cells were lysed with 6× SDS buffer for total protein analysis. Lysates were incubated for 12 h at 4°C with 25 μl Ni-nitrilotriacetic acid (Ni-NTA) agarose (Qiagen) prewashed with lysis buffer. The slurry was washed with lysis buffer and then with buffer A (8 M urea, 0.1 M Na_2HPO_4, 0.1 M NaH_2PO_4, 10 mM Tris-HCl, pH 8.0, 20 mM imidazole, and 5 mM β-mercaptoethanol) and with buffer B (8 M urea, 0.1 M Na_2HPO_4, 0.1 M NaH_2PO_4, 10 mM Tris-HCl, pH 6.3, 20 mM imidazole, and 5 mM β-mercaptoethanol). After denaturation, proteins were separated by SDS-PAGE, transferred to polyvinylidene difluoride (PVDF) membranes, and visualized by immunoblotting.

Quantitative RT-PCR analysis. Total RNA was isolated from U2OS cells by use of TRIzol reagent (Invitrogen) as described by the manufacturer. The amount of total RNA was measured, and 1 μg of RNA was reverse transcribed using a reverse transcription (RT) system from Promega. To amplify specific viral genes, the following primers were designed: 18S rRNA fwd primer, 5′-CGGCTACCACATCCAAGGAA-3′; 18S rRNA rev primer, 5′-GCTGGAATTACCGCGGCT-3′; E1A fwd primer, 5′-GTGCCCCATTAACCAGTTG-3′; E1A rev primer, 5′-GGCG TTTACAGCTCAAGTCC-3′; E2A fwd primer, 5′-GAAATTACGGTGAT GAACCCG-3′; E2A rev primer, 5′-CAGCCTCCATGCCCTTCTCC-3′; Fiber fwd primer, 5′-GGAGACAAAACTAAACCTGTAACAC-3′; and Fi-

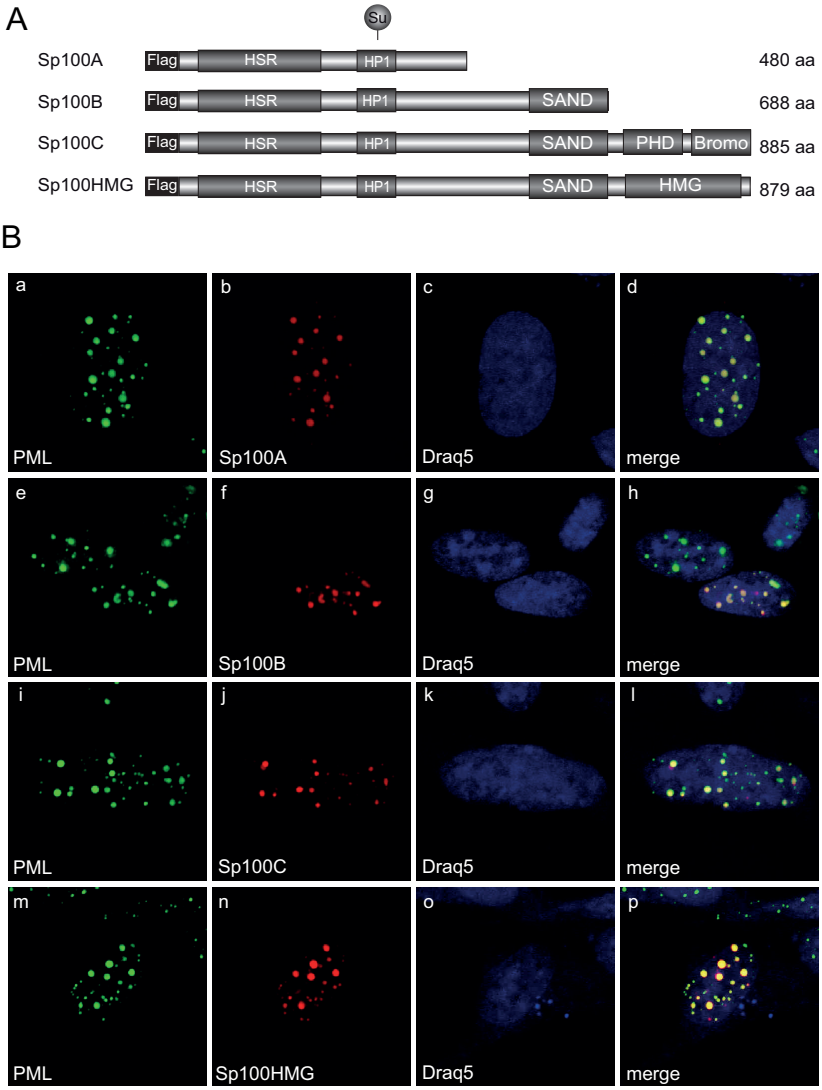

FIG 2 Localization of Sp100 isoforms in noninfected cells. (A) Schematic representation of N-terminally Flag-tagged Sp100 isoforms depicting their domain organization. HSR, homogenously stained region; HP1, heterochromatin protein 1 interaction region; SAND, Sp100, AIRE-1, NucP41/45, and DEAF-1 domain; bromo, bromodomain; PHD, plant homeodomain; HMG, high-mobility-group domain; Su, SUMO conjugation motif. Amino acid (aa) lengths are indicated on the right. (B) HepaRG cells were transfected with 1.5 μg of pFlag-Sp100A, -B, -C, or -HMG. Cells were fixed at 48 h posttransfection with 4% PFA and double labeled with MAb Flag-M2 (anti-Flag) and pAb NB 100-59787 (anti-PML). Primary Abs were detected with Cy3 (anti-Flag; red)- and Alexa 488 (anti-PML; green)-conjugated secondary Abs. The DNA-intercalating dye DRAQ5 (Biostatus) was used for nuclear staining. Anti-PML (green; panels a, e, i, and m) and anti-Flag-Sp100 (red; panels b, f, j, and n) staining patterns representative of at least 50 analyzed cells are shown. Overlays of the single images (merge) are shown in panels d, h, l, and p. Magnification, ×7,600.

ber rev primer, 5′-TCCCATGAAAATGACATAGAGTATGC-3′. Quantitative RT-PCR was performed with a first-strand method in a Rotor-Gene 6000 instrument (Corbett Life Sciences, Sydney, Australia), using 0.5-ml reaction tubes containing a 1/50 dilution of the cDNA template, 10 pmol/μl of each synthetic oligonucleotide primer, and 5 μl/sample SensiMix SYBR (Bioline). The PCR conditions were as follows: 10 min at 95°C followed by 40 cycles of 30 s at 95°C, 30 s at 62°C, and 30 s at 72°C. The average threshold cycle (C_T) value was determined from triplicate reactions, and levels of viral mRNA relative to cellular 18S rRNA were calculated. The identities of the products obtained were confirmed by melting curve analysis.

RESULTS

Sp100 depletion promotes Ad progeny production and early viral protein synthesis. To analyze the effect of Sp100 on Ad progeny production, we used human HepaRG cells, which have been reported to be susceptible to Ad5 infection (72) and represent a suitable system for analyzing PML-NB components during viral infection (73). After lentivirus transduction, endogenous Sp100 levels were efficiently depleted in HepaRG cells, as demonstrated by immunofluorescence and Western blot analyses (Fig. 1A and B) (55), whereas cell growth was not affected (Fig. 1C).

Compared to the case in parental cell lines (Hep par), knockdown of Sp100 increased the production of infectious virus particles 2-fold at 48 h p.i. (Fig. 1D). Additionally, we monitored expression of viral early and late proteins in HepaRG cells at different time points after infection and observed that expression of viral early proteins increased substantially in Sp100-depleted cells compared to the parental cells (data not shown).

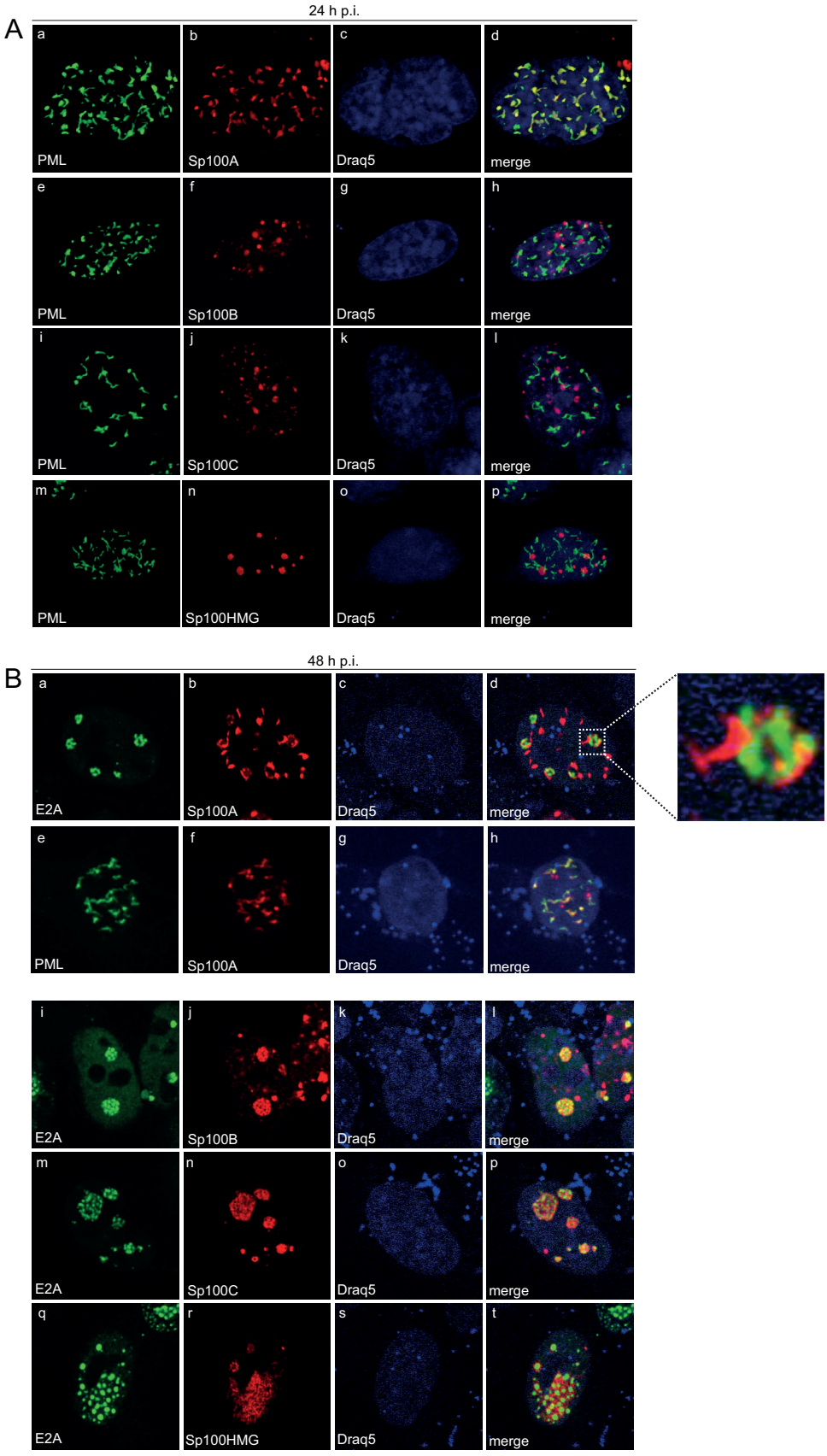
A
24 h p.i.
a
PML
b
Sp100A
c
Draq5
d
merge
e
PML
f
Sp100B
g
Draq5
h
merge
i
PML
j
Sp100C
k
Draq5
l
merge
m
PML
n
Sp100HMG
o
Draq5
p
merge
B
48 h p.i.
a
E2A
b
Sp100A
c
Draq5
d
merge
e
PML
f
Sp100A
g
Draq5
h
merge
i
E2A
j
Sp100B
k
Draq5
l
merge
m
E2A
n
Sp100C
o
Draq5
p
merge
q
E2A
r
Sp100HMG
s
Draq5
t
merge

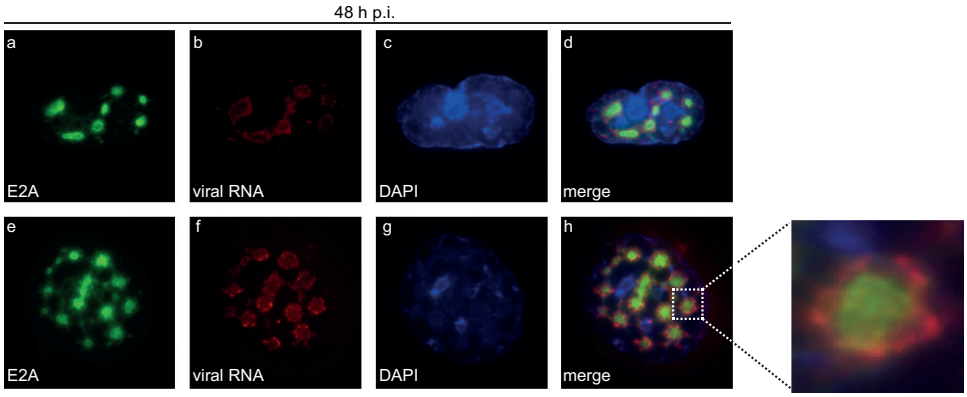

FIG 4 Ad mRNA surrounds viral replication centers. HepaRG cells were infected with wt virus (H5*pg*4100) at a multiplicity of infection of 10 FFU/cell. At 24 h p.i., cells were fixed and hybridized *in situ* as described in the text prior to labeling with mouse MAb anti-E2A. The primary Ab was detected with an Alexa 488 (anti-E2A; green)-conjugated secondary Ab. DAPI was used to stain nuclei. Staining patterns representative of at least 30 analyzed cells are shown. Overlays of the single images (merge) are shown in panels d and h. Magnification, ×7,600.

Sp100B, -C, and -HMG are relocalized from PML-NBs to viral replication centers during Ad infection. Humans are so far known to express at least four different Sp100 isoforms: Sp100A, Sp100B, Sp100C, and Sp100HMG. To investigate the intracellular localization of the different Sp100 isoforms in noninfected HepaRG cells, we transfected single Flag-tagged Sp100 isoforms (Fig. 2A) prior to immunofluorescence analysis. Costaining of Flag-tagged Sp100 isoforms with endogenous PML revealed localization of all Sp100 isoforms to PML-NBs (Fig. 2B). Although some PML-NBs seemed to lack Flag-Sp100B, -C, and -HMG staining in particular, and although higher expression levels induced the formation of larger nuclear aggregates, with an increased intensity of diffuse nuclear labeling, mild overexpression resulted in colocalization in at least about 50% of the detected PML-NBs. These observations are in line with the reports of Seeler and coworkers (11).

In 1996, Doucas and coworkers described the relocalization of endogenous Sp100 during Ad infection. In the early phase, PML and Sp100 are reorganized into so-called track-like structures prior to Sp100 being sequestered to the early viral replication centers (74). Therefore, we evaluated whether Sp100 colocalized to Ad-induced PML tracks or juxtaposed with established viral replication centers is affected in an isoform-dependent manner. HepaRG cells were transfected with the single Sp100 isoforms and superinfected with Ad wt virus (Fig. 3).

Intriguingly, we detected only the Sp100A isoform efficiently colocalizing with the PML-containing tracks (Fig. 3A, panel d). In contrast, Sp100B, Sp100C, and Sp100HMG formed dot-like structures not associated with PML ($n = 50$) (Fig. 3A, panels h, l, and p). After late replication centers, marked by the Ad DNA binding protein E2A-DBP (Fig. 3B, panels a, i, m, and q), were established at 48 h p.i., the majority of Sp100A was still retained in the PML-containing tracks (Fig. 3B, panels d and h). Our data revealed that a substantial number of these Ad-induced tracks were closely associated with the outer rims of the viral replication centers (Fig. 3B, panels b and d and inset), whereas Sp100B, -C, and -HMG accumulated entirely in the replication centers (Fig. 3B, panels l, p, and t). Based on these observations, we concluded that in contrast to Sp100A, the B, C, and HMG isoforms are separated from the PML tracks during Ad infection. This is likely due to different protein properties conferred by the additional C-terminal domains, e.g., the SAND domain.

Next, we investigated the subcellular location of *de novo*-synthesized viral RNA in relation to Ad replication centers. E2A was visualized by immunofluorescence staining after *in situ* hybridization with fiber-specific probes (Fig. 4). Our data show that viral RNA aggregated significantly at the periphery of the E2A-containing complexes (Fig. 4d and h). Additionally, we identified Sp100A encircling these E2A-labeled replication centers (Fig. 3B, panel d), colocalizing with arising PML tracks (Fig. 3B, panel h). We demonstrated conclusively that *de novo*-synthesized viral RNA was found mainly at the outer rims of Ad replication centers (Fig. 4) juxtaposed on PML tracks containing Sp100A (Fig. 3B). At the same time, Sp100B, -C, and -HMG were recruited to viral replication sites (Fig. 3B, panels l, p, and t) as seen for cellular restriction factors, such as the recently identified Ad repressor SPOC1 (75).

SUMO-2 chains of Sp100 are shortened during Ad infection. Since Ad apparently manipulates association of Sp100 isoforms with PML-NBs, we monitored whether SUMO modification of Sp100A is altered during infection. First, HeLa cells expressing His-SUMO-1 and -2 were transfected with Sp100A (Fig. 5A) and superinfected with wt Ad at 8 h posttransfection (Fig. 5A and B). Immunoblotting of Ni-NTA-purified His-SUMO conjugates

FIG 3 Ad-dependent relocalization of Sp100B, -C, and -HMG from PML-NBs to viral replication centers. HepaRG cells were transfected with 1.5 μg of pFlag-Sp100A, -B, -C, or -HMG and superinfected with wt virus (H5*pg*4100) at a multiplicity of infection of 50 FFU/cell at 8 h posttransfection. (A) The cells were fixed with 4% PFA at 24 h p.i. and double labeled with MAb Flag-M2 (anti-Flag) and pAb NB 100-59787 (anti-PML). (B) The cells were fixed with 4% PFA at 48 h p.i. and double labeled with MAb Flag-M2 (anti-Flag) and pAb NB 100-59787 (anti-PML) or rabbit MAb anti-E2A. Primary Abs were detected with Cy3 (anti-Flag; red)- and Alexa 488 (anti-PML/E2A; green)-conjugated secondary Abs. The DNA-intercalating dye DRAQ5 (Biostatus) was used to stain nuclei. Anti-PML (green; A, panels a, e, i, and m, and B, panel e), anti-E2A (green; B, panels a, i, m, and q), and anti-Flag-Sp100 (red; A, panels b, f, j, and n, and B, panels b, f, j, n, and r) staining patterns representative of at least 50 analyzed cells are shown. Overlays of the single images (merge) are shown in panels d, h, l, p, and t. Magnification, ×7,600.

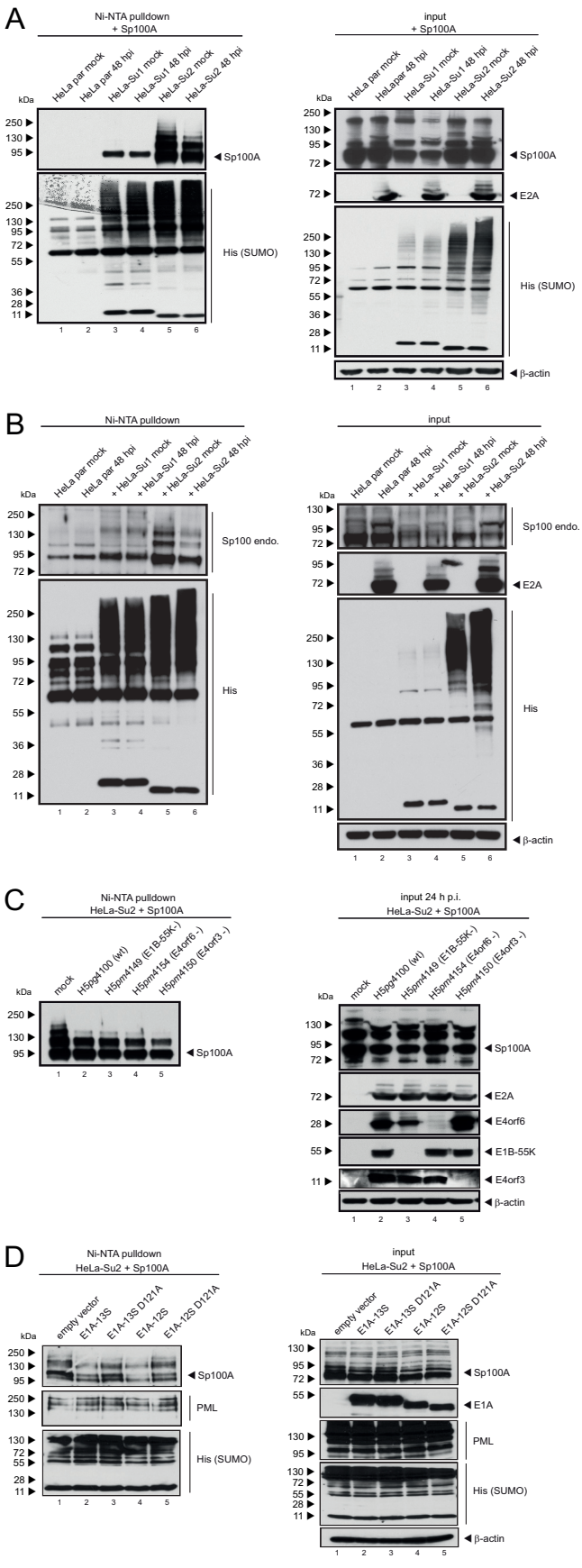

(Fig. 5A, left panel, lane 6) and crude lysates (Fig. 5A, right panel, lane 6) revealed that Sp100A SUMO-2 modification was reduced during Ad infection. However, SUMO-1 conjugation on Sp100A was not affected at this time point (Fig. 5A, left panel, lane 4). A similar effect could be observed for endogenous Sp100 (Fig. 5B).

To investigate whether the reduction of high-molecular-weight forms of SUMO-2-modified Sp100A depends on the viral early proteins E1B-55K, E4orf6, and/or E4orf3, His-SUMO-2 conjugates were purified (Ni-NTA) after Sp100A transfection and superinfection with wt virus or mutant viruses lacking either E1B-55K (H5*pm*4149), E4orf6 (H5*pm*4154), or E4orf3 (H5*pm*4150) (Fig. 5C). Significantly lower levels of high-molecular-weight SUMO-2-modified forms of Sp100 were detected with all viruses, irrespective of E4orf3, E1B-55K, or E4orf6 expression.

It has previously been shown that the viral early protein E1A represses SUMO modification of the retinoblastoma protein and interacts with the SUMO-conjugating enzyme Ubc9 to likely interfere with polySUMOylation (76, 77). Therefore, we tested if E1A triggers reduced SUMO-2 modification of Sp100 (Fig. 5D). As a control, we included Ubc9 binding mutants of the two major Ad5 E1A proteins, E1A-12S and E1A-13S (E1A-12S-D121A and E1A-13S-D121A mutants), with a point mutation in the conserved Ubc9 interacting motif (EVIDLT). This mutation has previously been shown to prevent E1A interaction with Ubc9 (Fig. 5D) (76). Analysis of Ni-NTA-purified SUMO-2 conjugates after coexpression of Sp100A with E1A-13S, E1A-13S-D121A, E1A-12S, and E1A-12S-D121A revealed that both wt E1A isoforms (Fig. 5D, left panel, lanes 2 and 4), but not the Ubc9 binding mutants (E1A-13S-D121A and E1A-12S-D121A), repressed SUMO-2 modification of Sp100A (Fig. 5D, left panel, lanes 3 and 5). We also noticed a slight reduction in steady-state levels of Sp100A after cotransfection with wt E1A-12S or E1A-13S and assumed that SUMO modification affects the stability of Sp100 (Fig. 5D, right panel, lanes 2 and 4). As a control, we included PML but could detect neither a change in steady-state levels nor a significant change in SUMO modification, implying a specific effect on Sp100. Since transfection of E1A-12S or -13S alone did not completely abolish Sp100 SUMO modification, it is likely that other viral regulatory proteins affect SUMO modification of Sp100 during infection.

HP1α interaction with Sp100A is reduced during Ad infection. Sp100 has been shown to interact with HP1 via its PXVXL

FIG 5 SUMO-2 chains of Sp100 are shortened during Ad infection. Parental HeLa cells and HeLa cells stably expressing 6His-SUMO-1 or 6His-SUMO-2 were transfected with 2 μg of pFlag-Sp100A and then superinfected with wt virus (H5*pg*4100) (A) or a mutant virus lacking E4orf3 (H5*pm*4150), E4orf6 (H5*pm*4154), or E1B-55K (H5*pm*4149) (C) at a multiplicity of infection of 20 FFU/cell at 8 h posttransfection, as indicated, or cotransfected with 3 μg E1A-13S, E1A-12S, E1A-13S-D121A, or E1A-13S-D121A (D). (B) To monitor endogenous Sp100 (Sp100 endo.), the cells were infected with wt virus (H5*pg*4100) at a multiplicity of infection of 20 FFU/cell without transfection. For panels A to C, whole-cell lysates were prepared with guanidinium chloride buffer at 48 h posttransfection, subjected to Ni-NTA purification of 6His-SUMO conjugates, and fractionated in a 4 to 12% gradient gel before immunoblot analysis. Input levels of whole-cell lysates and Ni-NTA-purified proteins were detected using pAb GH3 (anti-Sp100), pAb PML NB100-59787, MAb M-58 (anti-E1A), MAb B6 (anti-E2A), MAb 6×His, MAb Flag-M2 (anti-Flag), MAb AC-15 (anti-β-actin), MAb 2A6 (anti-E1B-55K), MAb RSA3 (anti-E4orf6), and MAb 6A11 (anti-E4orf3). Molecular masses in kDa are indicated on the left, and specific proteins are indicated on the right.

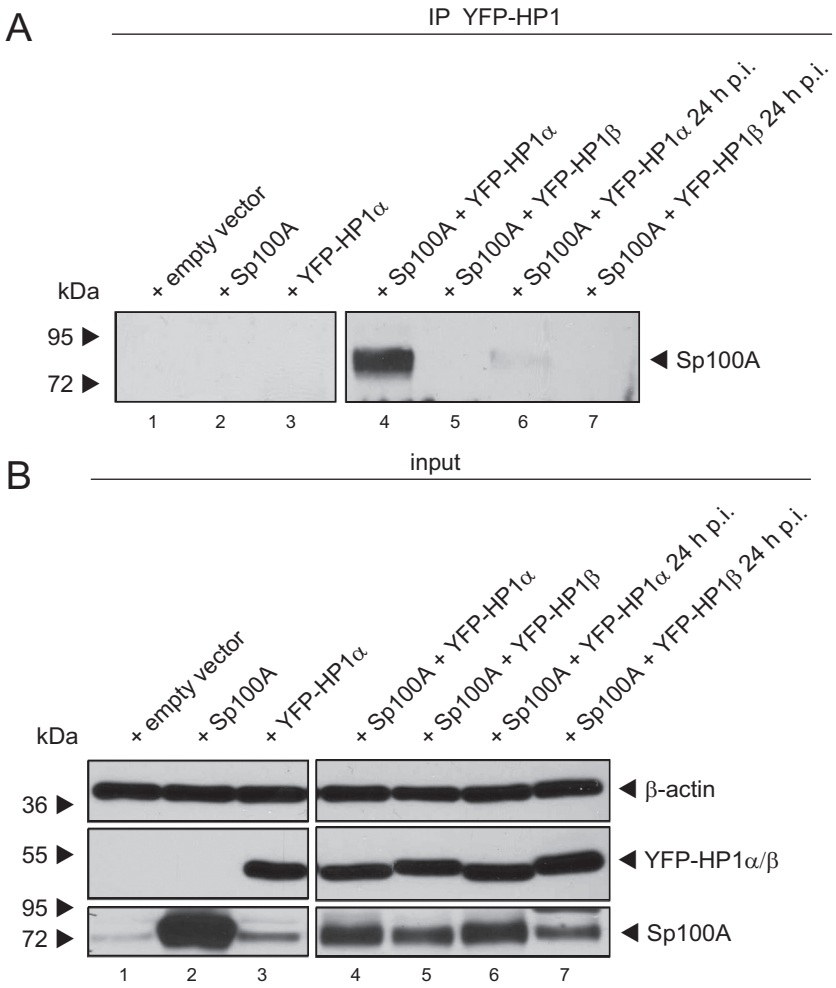

FIG 6 HP1α interaction with Sp100A is reduced during Ad infection. H1299 cells were superinfected with wt virus (H5*pg*4100) at a multiplicity of infection of 20 FFU/cell 8 h after transfection of 2 μg of pFlag-Sp100A mutant and 3 μg of pYFP-HP1α/pYFP-HP1β, as indicated. Cells were harvested at 24 h p.i., prior to preparation of coimmunoprecipitation (IP) samples and whole-cell extracts. Coprecipitated proteins (A) and input levels (B) of whole-cell lysates were detected using pAb GH3 (anti-Sp100), AC-15 (anti-β-actin), and YFP antibody (anti-YFP-HP1α/pYFP-HP1β). Molecular masses in kDa are indicated on the left, and specific proteins are indicated on the right.

motif (18). Overexpressed or IFN-induced Sp100 enhances recruitment of endogenous HP1 protein to PML-NBs, mainly localizing to the interior of these subdomains (18, 46). Additionally, the Sp100 SUMO conjugation site (SCS) is located close to the HP1 interaction motif, and SUMOylated Sp100 is known to stabilize its binding to HP1 *in vitro* (11). To test whether Ad-mediated loss of Sp100A-SUMO-2 affects the HP1 interaction *in vivo*, we performed binding assays with infected, Sp100A-overexpressing cells cotransfected with either HP1α or HP1β (Fig. 6). We could not detect an interaction between Sp100A and HP1β. However, we noticed that HP1α binding to Sp100A was significantly reduced in infected cells (Fig. 6A, lane 6).

Sp100A-specific activation of Ad promoter activity. Recently, Newhart et al. reported that Sp100A promotes chromatin decondensation at cytomegalovirus (CMV) promoter-regulated transcription sites. In contrast, Sp100B, containing an additional SAND domain, promotes chromatin condensation, and thus transcriptional repression (20). To test whether Sp100 also affects transcription from Ad promoters, we investigated Ad E1A, E2early, pIX, and E3 promoter activity in the presence of either Sp100A or Sp100B, as stable knockdown of each isoform was not feasible due to sequence similarity (Fig. 7).

Since Sp100A was recently reported not to overcome Daxx/ATRX-mediated transcriptional repression (20), we used U2OS cells, which have reduced ATRX expression, to minimize additional effects mediated by these transcription factors. Furthermore, we employed Daxx-depleted U2OS cells (78) to additionally diminish the repressive effect of the Daxx-ATRX chromatin remodeling complex. We observed that Sp100A stimulated transcription from the Ad promoters ~2- to 3-fold in both cell lines. As anticipated, basal activity of the promoters was higher in Daxx-depleted cells, implying an additional repression mechanism of Daxx that is independent of the Daxx-ATRX complex. In contrast to Sp100A, the B isoform reduced E2early, pIX, and E3 promoter activity ~0.5- to 3-fold (Fig. 7A).

Additionally, we measured *Renilla* luciferase activity under the control of the HSV-TK promoter, which is normally used as an internal normalization control. We observed that Sp100 also af-

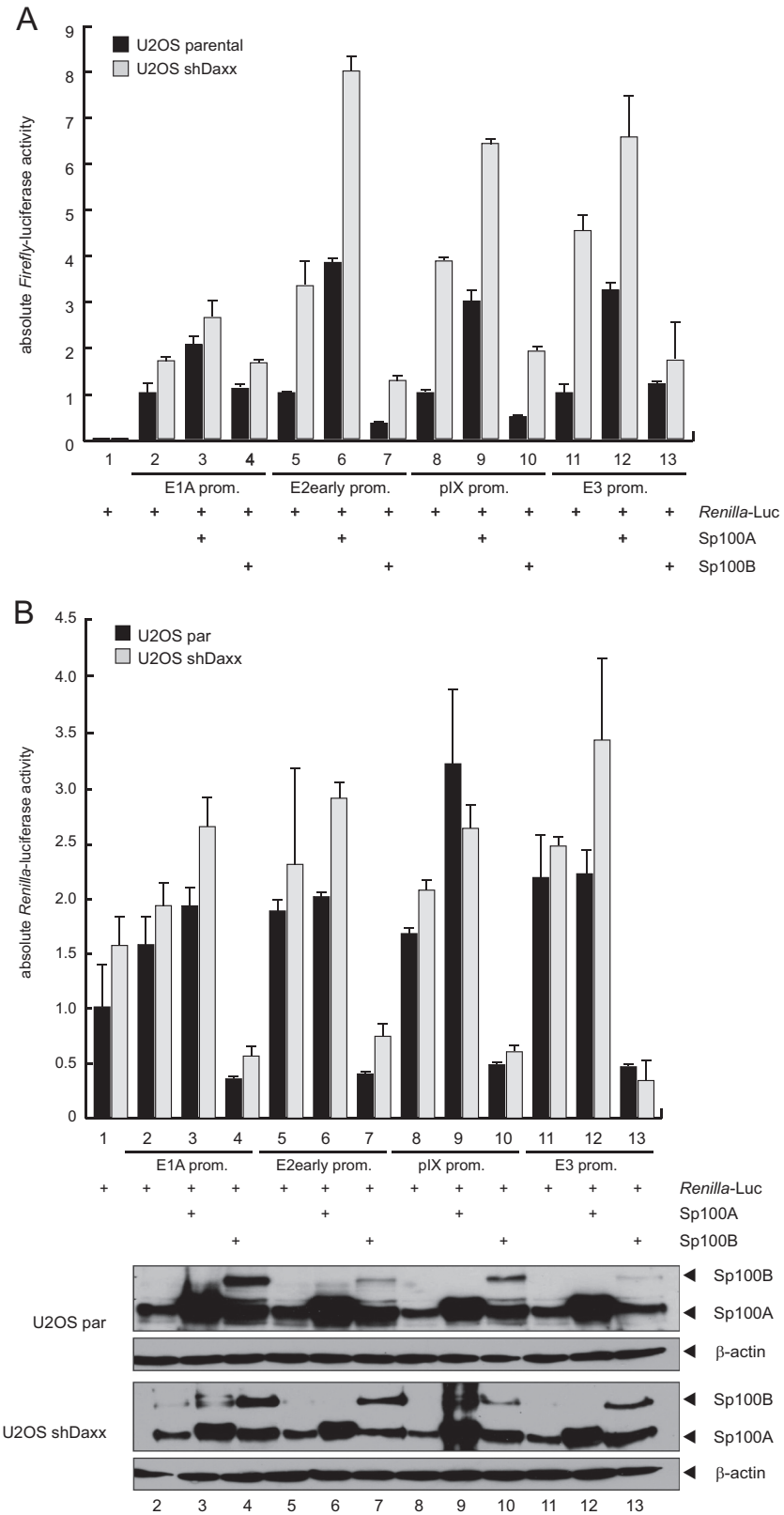

FIG 7 Sp100 isoform-specific regulation of Ad gene expression. (A) U2OS and U2OS shDaxx cells were transfected with 0.5 μg p*Renilla*-Luc, 0.5 μg pGL-E1A-promoter, pGL-E2early-promoter, pGL-E3-promoter, or pGL-pIX-promoter, and 0.5 μg pSp100A or pSp100B in the combinations indicated (+). Total cell extracts were prepared and luciferase activities determined at 24 h posttransfection. Absolute firefly luciferase activities are shown. Means and standard deviations for two independent experiments are presented. (B) Means and standard deviations of absolute *Renilla* luciferase activities are presented for two independent experiments. Input levels of total cell lysates were detected using pAb GH3 (anti-Sp100) and MAb AC-15 (anti-β-actin).

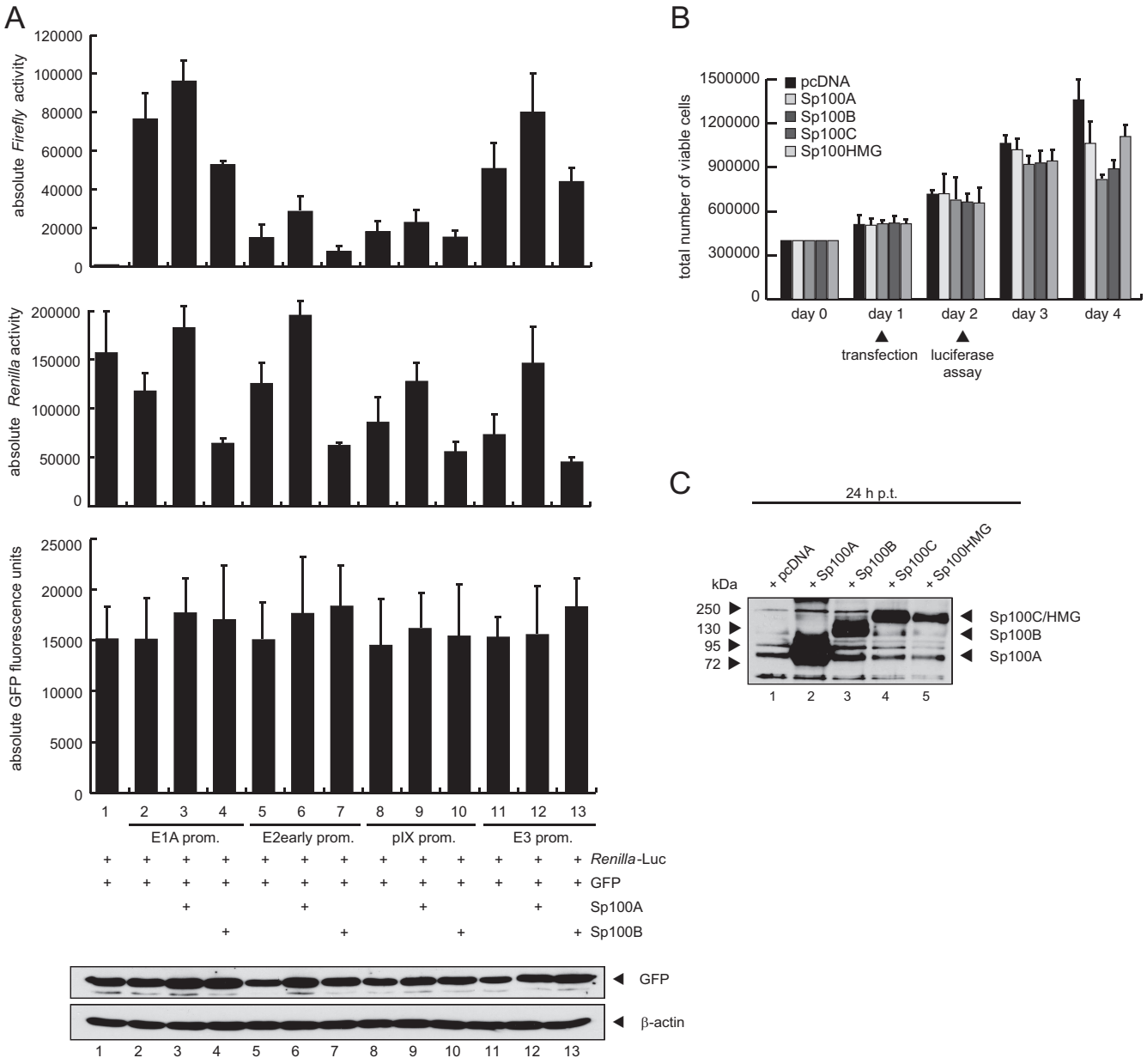

FIG 8 Differences in transfection efficiency do not account for the Sp100 isoform-specific effect on gene expression. (A) U2OS cells were transfected with 0.5 μg p*Renilla*-Luc, 0.5 μg pGFP, 0.5 μg pGL-E1A-promoter, pGL-E2early-promoter, pGL-E3-promoter, or pGL-pIX-promoter, and 0.5 μg pSp100A or pSp100B in the combinations indicated (+). GFP fluorescence signals were measured using a Tecan Infinite 200 Pro plate reader before total cell extracts were prepared and luciferase activities determined at 24 h posttransfection. Absolute firefly luciferase activities and *Renilla* luciferase activities are shown. Means and standard deviations for three independent experiments are presented. Input levels of total cell lysates were detected using MAb AC-15 (anti-β-actin) and a GFP epitope MAb. (B) U2OS cells were transfected with 3 μg of pcDNA, pSp100A, or pSp100B, and total cell numbers were determined by trypan blue exclusion at the indicated time points. Time points of transfection and luciferase assay are indicated at the bottom. (C) U2OS cells were transfected with 3 μg of pcDNA, pSp100A, or pSp100B, and total cell extracts were prepared at 24 h posttransfection. Proteins were separated by SDS-PAGE and subjected to immunoblotting using pAb GH3 (anti-Sp100).

fected *Renilla* luciferase expression, either transactivating it via Sp100A or repressing it via Sp100B (Fig. 7B).

Such effector-dependent activation or repression of control genes included for normalization was previously reported by other groups and was circumvented by use of a GFP expression vector for internal transfection control (79–81). Hence, we included a GFP-expressing vector as an additional control to determine transfection efficiencies (Fig. 8A) as previously described (82). In contrast to the *Renilla* luciferase activity, the GFP signal was not increased by coexpression of Sp100A or decreased by Sp100B (Fig. 8A). This was also validated by immunoblot analysis of the crude extracts (Fig. 8A, bottom panel).

Furthermore, we monitored cell growth of the U2OS cells via trypan blue exclusion after transfection of Sp100A, -B, -C, or -HMG or an empty vector to exclude that changes in cell viability account for the different effects of the Sp100 isoforms on lucifer-

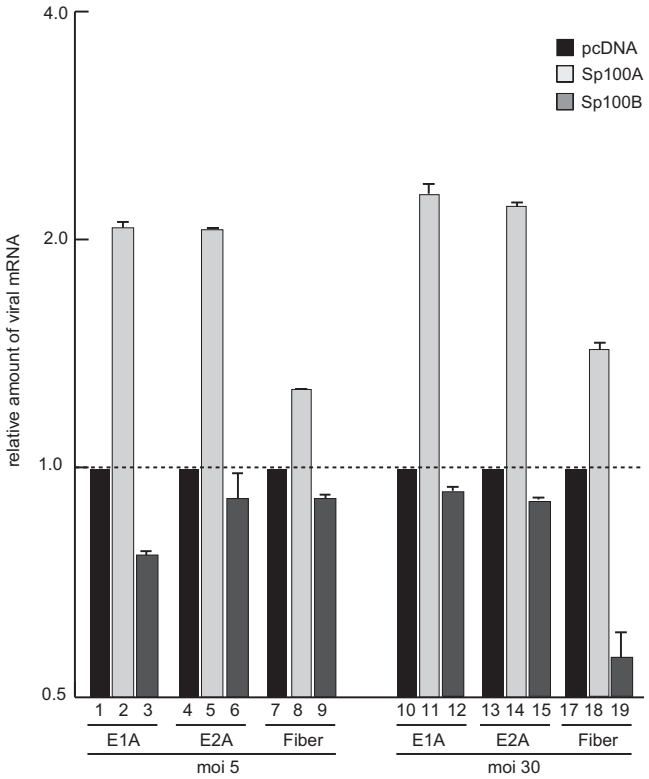

FIG 9 Sp100 isoform-specific regulation of Ad mRNA synthesis. Subconfluent U2OS cells were transfected with 5 μg pcDNA, pSp100A, or pSp100B and superinfected with wild-type virus (H5*pg*4100) at a multiplicity of infection (MOI) of 5 or 30 FFU/cell at 48 h posttransfection. The cells were harvested at 24 h p.i., and total RNA was extracted, reverse transcribed, and quantified by RT-PCR analysis using primers specific for Ad5 E1A, E2A, and fiber. The data were normalized to 18S rRNA levels. The data are presented on a log axis relative to the amount of RNA detected in control cells expressing empty vector.

ase gene expression (Fig. 8B). Cell growth was not altered upon transfection of the Sp100 isoforms compared to the empty vector control until 72 h posttransfection. Since the reporter gene assays were performed at 24 h posttransfection, changes in cell viability after transfection of the Sp100 isoforms can be excluded for the time point of luciferase assay measurement (Fig. 8B). In addition, we also compared exogenous Sp100 protein expression at 24 h posttransfection, a time point equal to that of the reporter assays presented above (Fig. 8C).

To further confirm our data with the virus background, we measured Ad early and late mRNA expression in infected cells expressing either Sp100A or Sp100B (Fig. 9). Viral early E1A and E2A mRNA production was stimulated in infected cells expressing Sp100A compared to cells treated with the empty vector control (Fig. 9). Additionally, late fiber transcript synthesis was enhanced in cells cotransfected with Sp100A, suggesting an impact of either enhanced synthesis of early viral gene products or direct stimulation of the late promoter (Fig. 9). Consistent with data obtained in the reporter assays described above, Sp100B negatively affected viral early and late mRNA expression, although the effect was not as strong as that observed for Sp100A-dependent activation. Similar results were obtained for early and late mRNA stimulation by Sp100A in cells infected at a higher multiplicity of infection (Fig. 9).

The Sp100A SIM promotes transcriptional activation and localization to track-like structures. The transactivating properties of Sp100 on transcription have previously been mapped to amino acids 333 to 407, a region immediately downstream of the HP1 interaction region (9). The SUMO-interacting motif (SIM) has been described to be important for Sp100 recruitment to HSV-1 genomes (83). Given the fact that the SIM is located within the transactivating region of Sp100, we investigated the transcriptional properties of an Sp100A nonfunctional SIM derivative (Sp100A-I323I324K) on Ad promoters (Fig. 10A). Reporter gene assays with the Ad E2early promoter revealed that the Sp100A-SIM mutant was no longer able to efficiently stimulate transcription from the viral promoter (Fig. 10A, lane 7), although Sp100A-wt and the Sp100A-SIM mutant were expressed in similar amounts (Fig. 10A, lower panel).

Next, we tested whether the SIM mutation would alter the intracellular localization of Sp100A (Fig. 10B). In noninfected cells, the Sp100A-SIM mutant localized to the PML-NBs (Fig. 10B). Costaining with Ad E2A-DBP revealed that after PML track formation, the Sp100A-SIM mutant was diffusely distributed in the host cell nucleus, localizing neither to the tracks nor to the viral replication centers in 80% of the cells investigated ($n > 50$) (Fig. 10B, panels h and m). However, in 20% of the cells, the Sp100A-SIM mutant localized to PML tracks and/or viral replication centers, likely due to dimerization with endogenous wt Sp100 via the HSR domain ($n > 50$) (data not shown).

DISCUSSION

Nuclear-replicating DNA viruses antagonize intrinsic antiviral defense mechanisms to replicate efficiently; however, the functional mechanisms behind this phenomenon are diverse and not well understood. Here we unravel some more pieces of the puzzle, using Ad as a model virus, and propose a novel Ad evasion strategy that involves isoform-specific, active manipulation of the host restriction factor Sp100 as a prerequisite for efficient viral replication.

Initial experiments demonstrated that during the first hours of Ad infection, E1A orchestrates the temporally regulated expression of viral proteins. Simultaneously, the early adenoviral proteins E1B-55K and E4orf3 are expressed (84). First, E4orf3 induces the reorganization of PML nuclear bodies by interacting with PML-II, which leads to the formation of track-like structures in the nuclei of cells (Fig. 11) (74, 85–90). This reorganization of PML-NBs is highly conserved among most Ad species (91) and therefore suggests an important function during Ad infection, presumably in eliminating intracellular viral defense barriers (35, 37, 74, 92). In parallel, SUMOylated E1B-55K is localized to the PML-NBs, presumably by interacting with PML-IV (93). Notably, the presence of E4orf3 and E1B-55K synergistically modulates p53 transcriptional activity (94), which might come about by altering PML-IV function and consequently inducing E1B-55K-dependent SUMOylation of the p53 protein (95, 96). During the onset of viral infection, E4orf6, which is expressed with a delay of 6 h compared to E1B-55K/E4orf3, facilitates nuclear matrix release of E1B-55K via deSUMOylation (93). Finally, E1B-55K–E4orf6 complex formation induces proteasomal degradation of repressive factors, such as p53, ATRX, and SPOC1 (Fig. 11) (97–101).

Based on available data obtained with different DNA viruses, it is reasonable to conclude that diverse molecular mechanisms have evolved to counteract PML-NB-mediated antiviral activities. In-

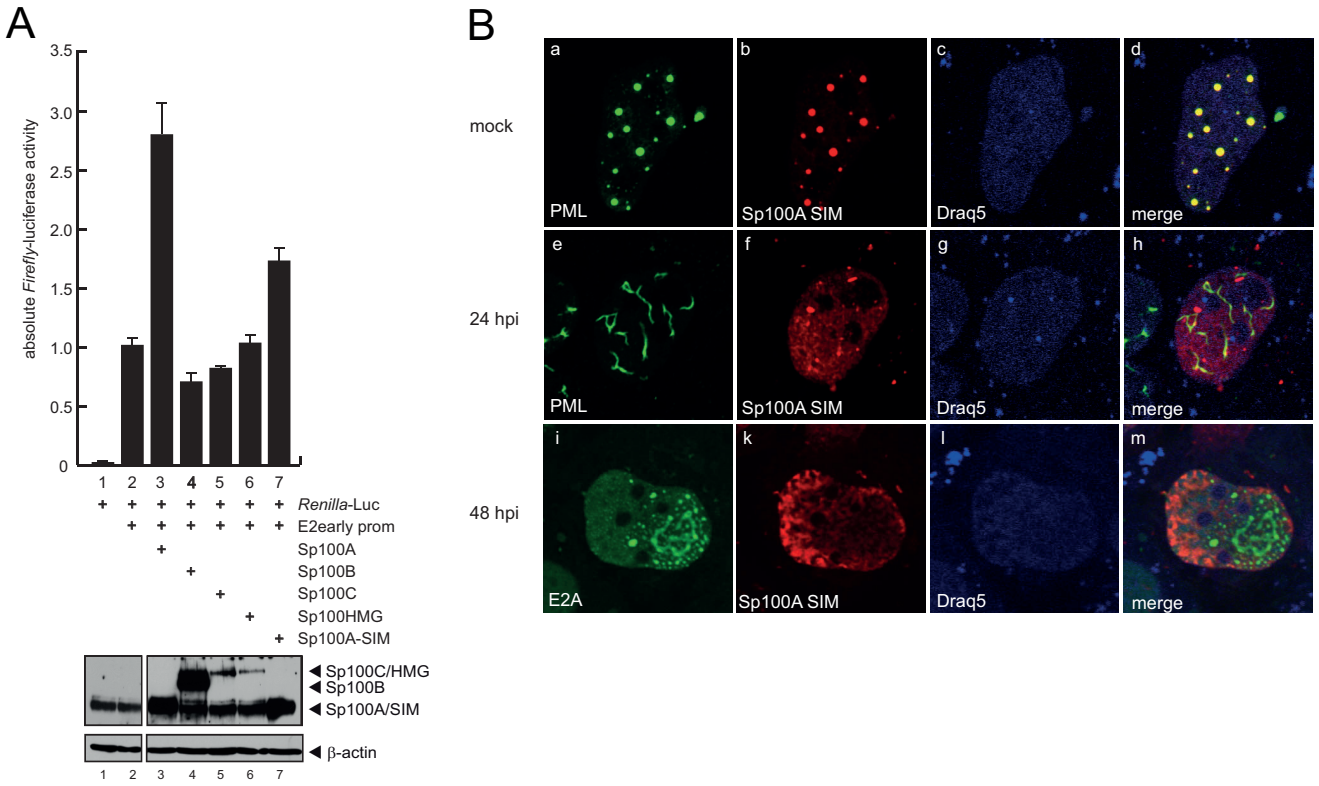

FIG 10 Sp100A transcriptional activation and localization depend on a functional SIM. (A) U2OS cells were transfected with 0.5 μg p*Renilla*-Luc, 0.5 μg pGL-E2early-promoter, and 0.2 μg pE1A-13S, pSp100A, pSp100B, pSp100C, pSp100HMG, or pSp100A-SIM in the combinations indicated (+). Absolute firefly luciferase activities are shown, with means and standard deviations for three independent experiments. Data are presented uncorrected for transfection controls as explained in the legend to Fig. 8. Input levels of total cell lysates were detected using pAb GH3 (anti-Sp100) and MAb AC-15 (anti-β-actin). (B) HepaRG cells were transfected with 1.5 μg of pFlag-Sp100A SIM and superinfected with wild-type virus (H5*pg*4100) at a multiplicity of infection of 50 FFU/cell at 8 h posttransfection. The cells were fixed with 4% PFA at 48 h p.i. and double labeled with pAb NB 100-59787 (anti-PML), MAb Flag-M2 (anti-Flag), and rabbit MAb anti-E2A. Primary Abs were detected with Cy3 (anti-Flag; red)- and Alexa 488 (anti-E2A; green)-conjugated secondary Abs. The DNA-intercalating dye DRAQ5 (Biostatus) was used for nuclear staining. Anti-PML (green; panels a and e), anti-E2A (green; panel i), and anti-Flag-Sp100 (red; panels b, f, and k) staining patterns representative of at least 50 analyzed cells are shown. Overlays of the single images (merge) are shown in panels d, f, and m. Magnification, ×7,600.

activation of PML-NBs during early stages of HSV-1 infection depends exclusively on the expression of the immediate early protein ICP0, which rapidly localizes to these subnuclear structures and disrupts them completely (102–107). Interestingly, ICP0 leads to the rapid loss of high-molecular-weight PML in a proteasome-dependent manner, and subsequently results in disintegration of PML-NB structures (108, 109). Since ICP0-mediated proteasomal depletion also includes the PML-NB-associated protein Sp100, it has been suggested that degradation occurs via interference with a common SUMOylation pathway rather than by specific targeting of individual proteins (110). Another study provides evidence that the formation of repressive PML-NB-like structures in association with incoming viral DNA depends on the respective SIMs of antiviral proteins, such as PML, Sp100, and Daxx (111). This observation provides a convincing explanation for how early viral proteins may inhibit the antiviral functions of these proteins by depleting PML-SUMO conjugates and, consequently, eliminating their SIM-dependent recruitment.

For Ad, the functional consequences of E4orf3-induced PML-NB reorganization prior to formation of track-like structures in the nuclei of cells still remain unclear. However, here we provide evidence that Ad selectively counteracts antiviral immune responses and, at the same time, benefits from other PML-NB-associated components by actively recruiting them to PML track-like structures, the sites of viral transcription in the host cell nucleus. Depletion of the PML-associated factor Sp100 results in significantly increased Ad progeny production (Fig. 1). According to our data, Ad counteracts this antiviral measure by specifically targeting the repressive isoforms Sp100B, Sp100C, and Sp100HMG. However, the negative impact of the B, C, and HMG isoforms together seems to be more potent in the repression of Ad replication than the activating effect of Sp100A, as knockdown of all isoforms causes an overall negative effect of the PML-NB component Sp100.

The transcription factor Sp100 has been reported to modulate the replication programs of several DNA viruses. Human CMV (HCMV) and herpesvirus saimiri (HVS) target Sp100 for proteasomal degradation; depletion of Sp100 by RNA interference enhances HCMV replication and gene expression (83, 112, 113). Similar to our findings, Maul and coworkers previously demonstrated that Sp100 isoforms B, C, and HMG, but not Sp100A, suppressed HSV-1 immediate early gene expression and repressed the ICP0 promoter and that this was dependent on the SAND domain (114). In 1996, Doucas et al. had already described Ad-dependent relocalization of endogenous Sp100 into the E4orf3-induced track-like PML structures at early times postinfection (74). During late stages, PML and Sp100 segregation was ob-

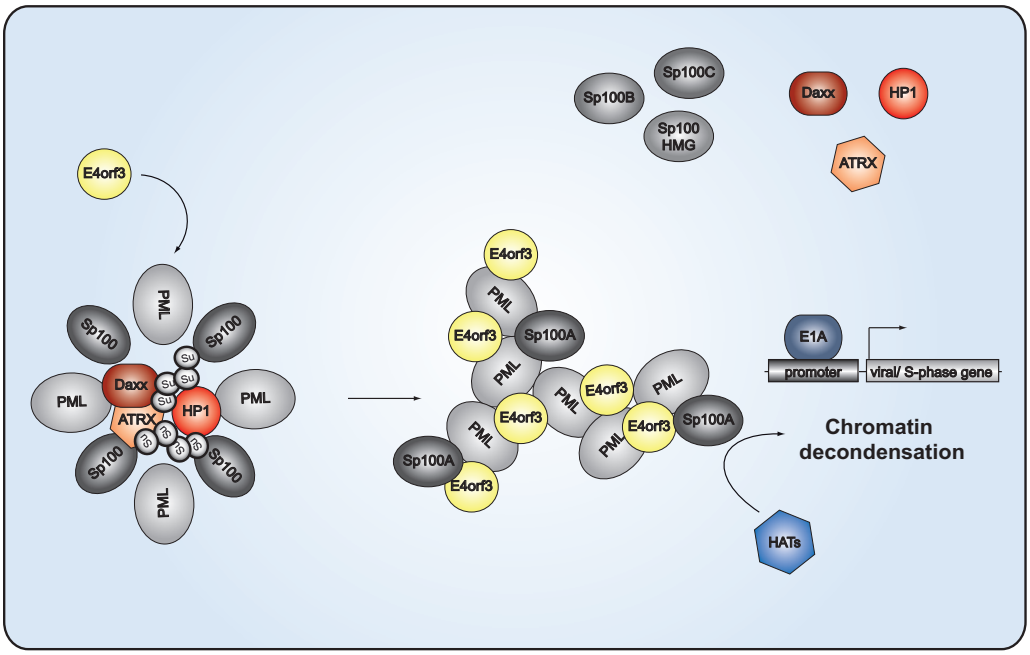

FIG 11 PML-NB-mediated transcriptional regulation of Ad gene expression. The schematic representation depicts the proposed model of Ad-mediated relocalization of antiviral factors associated with PML nuclear bodies. In noninfected cells, transcriptional activators and repressors, such as the Sp100 isoforms, HP1, Daxx, and ATRX, are clustered within the PML-NBs. Sp100A promotes chromatin decondensation and histone acetyltransferase (HAT) recruitment, whereas Sp100B, Sp100C, and Sp100HMG prevent these events. HP1 and the Daxx-ATRX complex function in gene silencing by organizing higher-order chromatin structures. Poly-SUMO-2/3 (Su) chains protrude into the interior of the PML-NB to mediate interactions with the HP1, Daxx, or ATRX enriched there. At early time points after infection, E4orf3 targets PML isoform II to reorganize PML-NB into track-like structures. SUMO-2/3 chains are shortened, causing release of the repressive factors HP1, Daxx, and ATRX from the PML-NBs. Under these conditions, Sp100A, associating with the PML tracks, is able to recruit HATs, thereby creating a favorable environment for activation of Ad gene expression.

served, with Sp100 relocalizing from these Ad-induced tracks to the early viral replication centers (114). Our novel findings now illustrate that the activating transcription isoform Sp100A is found mainly at the Ad-induced PML tracks, while only the repressive Sp100B, -C, and -HMG proteins are displaced from these nuclear structures to the Ad replication centers (Fig. 3 and 11). Besides these repressive Sp100 variants, other repressive factors or proteins participating in the DNA damage response (DDR) were already shown to be recruited to these nuclear loci, suggesting a common phenomenon during Ad infection (74). Based on our results, we believe that Ad-dependent loss of PML-NB integrity by redistribution into track-like structures consequently induces the dispersal of PML-associated repressive transcription factors in the nucleus. These antiviral proteins, e.g., Daxx, ATRX, and p53, are immediately targeted by the newly synthesized viral gene products (Fig. 11).

As described for herpesviruses (112, 115, 116), we observed modulation of SUMOylated Sp100 forms during Ad infection, a prerequisite for altered intranuclear localization of the different Sp100 proteins. Indeed, we observed that Sp100A activates transcription from Ad promoters (Fig. 7 to 9), most likely when it is kept at the PML tracks, where it may recruit histone acetylases to create a favorable environment for Ad gene expression (Fig. 11).

It has been proposed that HP1 and Sp100 form a SUMO-dependent complex to regulate chromatin remodeling (110), although the exact functionality of the complex is still unknown. HP1 proteins are phosphorylated in response to DNA damage and appear to be important for recruiting DDR factors and dynamically reorganizing chromatin (3, 117). For Epstein-Barr virus (EBV), EBNA-LP, the coactivator of the EBV transactivator EBNA2, has been shown to interact with Sp100 and to displace the Sp100-HP1α complex from PML-NBs (118). Consistent with these observations, Ad disrupts the Sp100-HP1α interaction, likely inducing chromatin decondensation (Fig. 6). Ad disrupts this interaction, suggesting that this cellular chromatin remodeling complex is repressive for virus replication by chromatin condensation, providing evidence for the general model that Ad promotes deSUMOylation of PML-NB-associated proteins to prevent recruitment of certain repressive factors to the PML track-like structures in infected cells (Fig. 11). This is further supported by the fact that poly-SUMO-2/3 chains protrude into the interior of PML-NBs, where they mediate the enriched interactions with HP1, Daxx, or ATRX.

The predominant opinion in the field is that PML-NBs are part of an IFN-induced antiviral defense mechanism (36–38, 119). However, new evidence also points to a proviral function (35). Specifically, DNA viruses require PML-NBs and associated proteins to establish efficient replication and transcription. We now show that this concept is more intricate than originally believed, since viruses apparently take advantage of specific PML-NB-associated proteins to actively establish a proviral environment in the host cell, while eliminating and inhibiting repressive factors. Simultaneously, antiviral measures are efficiently inhibited to maintain the viral infectious program. Obviously, ongoing studies on virus-host interactions and future insights into novel immune evasion strategies acquired by pathogenic viruses will contribute to identifying new therapeutic strategies and targets to limit or prevent virus-mediated diseases and mortality of patients.

ACKNOWLEDGMENTS

We thank Roger Everett and Hans Will for kindly providing reagents, and we greatly appreciate the critical comments and scientific discussions of Gregory Fonseca and Nicole Fischer.

The Heinrich Pette Institute, Leibniz Institute for Experimental Virology, is supported by the Freie und Hansestadt Hamburg and the Bundesministerium für Gesundheit (BMG). S.S. was supported by the Peter und Traudl Engelhorn Stiftung and additional grants from the Erich und Gertrud Roggenbuck Stiftung and the Else Kröner-Fresenius Stiftung. T.D. was supported by the Deutsche Forschungsgemeinschaft (DFG) and the Wilhelm Sander Stiftung. Part of this work was supported by the B. Braun Stiftung and the Fonds der Chemischen Industrie.

REFERENCES

1. **Guldner HH, Szostecki C, Grotzinger T, Will H.** 1992. IFN enhance expression of Sp100, an autoantigen in primary biliary cirrhosis. J. Immunol. **149:**4067–4073.
2. **Grotzinger T, Sternsdorf T, Jensen K, Will H.** 1996. Interferon-modulated expression of genes encoding the nuclear-dot-associated proteins Sp100 and promyelocytic leukemia protein (PML). Eur. J. Biochem. **238:**554–560. http://dx.doi.org/10.1111/j.1432-1033.1996.0554z.x.
3. **Lehming N, Le Saux A, Schuller J, Ptashne M.** 1998. Chromatin components as part of a putative transcriptional repressing complex. Proc. Natl. Acad. Sci. U. S. A. **95:**7322–7326. http://dx.doi.org/10.1073/pnas.95.13.7322.
4. **Szostecki C, Guldner HH, Netter HJ, Will H.** 1990. Isolation and characterization of cDNA encoding a human nuclear antigen predominantly recognized by autoantibodies from patients with primary biliary cirrhosis. J. Immunol. **145:**4338–4347.
5. **Szostecki C, Krippner H, Penner E, Bautz FA.** 1987. Autoimmune sera recognize a 100 kD nuclear protein antigen (sp-100). Clin. Exp. Immunol. **68:**108–116.
6. **Szostecki C, Will H, Netter HJ, Guldner HH.** 1992. Autoantibodies to the nuclear Sp100 protein in primary biliary cirrhosis and associated diseases: epitope specificity and immunoglobulin class distribution. Scand. J. Immunol. **36:**555–564. http://dx.doi.org/10.1111/j.1365-3083.1992.tb03224.x.
7. **Pandolfi PP, Alcalay M, Fagioli M, Zangrilli D, Mencarelli A, Diverio D, Biondi A, Lo Coco F, Rambaldi A, Grignani F.** 1992. Genomic variability and alternative splicing generate multiple PML/RAR alpha transcripts that encode aberrant PML proteins and PML/RAR alpha isoforms in acute promyelocytic leukaemia. EMBO J. **11:**1397–1407.
8. **Fagioli M, Alcalay M, Pandolfi PP, Venturini L, Mencarelli A, Simeone A, Acampora D, Grignani F, Pelicci PG.** 1992. Alternative splicing of PML transcripts predicts coexpression of several carboxy-terminally different protein isoforms. Oncogene **7:**1083–1091.
9. **Xie K, Lambie EJ, Snyder M.** 1993. Nuclear dot antigens may specify transcriptional domains in the nucleus. Mol. Cell. Biol. **13:**6170–6179.
10. **Dent AL, Yewdell J, Puvion-Dutilleul F, Koken MH, de The H, Staudt LM.** 1996. LYSP100-associated nuclear domains (LANDs): description of a new class of subnuclear structures and their relationship to PML nuclear bodies. Blood **88:**1423–1426.
11. **Seeler JS, Marchio A, Losson R, Desterro JM, Hay RT, Chambon P, Dejean A.** 2001. Common properties of nuclear body protein SP100 and TIF1alpha chromatin factor: role of SUMO modification. Mol. Cell. Biol. **21:**3314–3324. http://dx.doi.org/10.1128/MCB.21.10.3314-3324.2001.
12. **Guldner HH, Szostecki C, Schroder P, Matschl U, Jensen K, Luders C, Will H, Sternsdorf T.** 1999. Splice variants of the nuclear dot-associated Sp100 protein contain homologies to HMG-1 and a human nuclear phosphoprotein-box motif. J. Cell Sci. **112:**733–747.
13. **Sternsdorf T, Jensen K, Reich B, Will H.** 1999. The nuclear dot protein sp100, characterization of domains necessary for dimerization, subcellular localization, and modification by small ubiquitin-like modifiers. J. Biol. Chem. **274:**12555–12566. http://dx.doi.org/10.1074/jbc.274.18.12555.
14. **Bottomley MJ, Collard MW, Huggenvik JI, Liu Z, Gibson TJ, Sattler M.** 2001. The SAND domain structure defines a novel DNA-binding fold in transcriptional regulation. Nat. Struct. Biol. **8:**626–633. http://dx.doi.org/10.1038/89675.
15. **Isaac A, Wilcox KW, Taylor JL.** 2006. SP100B, a repressor of gene expression preferentially binds to DNA with unmethylated CpGs. J. Cell. Biochem. **98:**1106–1122. http://dx.doi.org/10.1002/jcb.20841.
16. **Fish PV, Filippakopoulos P, Bish G, Brennan PE, Bunnage ME, Cook AS, Federov O, Gerstenberger BS, Jones H, Knapp S, Marsden B, Nocka K, Owen DR, Philpott M, Picaud S, Primiano MJ, Ralph MJ, Sciammetta N, Trzupek JD.** 2012. Identification of a chemical probe for bromo and extra C-terminal bromodomain inhibition through optimization of a fragment-derived hit. J. Med. Chem. **55:**9831–9837. http://dx.doi.org/10.1021/jm3010515.
17. **Baker LA, Allis CD, Wang GG.** 2008. PHD fingers in human diseases: disorders arising from misinterpreting epigenetic marks. Mutat. Res. **647:**3–12. http://dx.doi.org/10.1016/j.mrfmmm.2008.07.004.
18. **Seeler JS, Marchio A, Sitterlin D, Transy C, Dejean A.** 1998. Interaction of SP100 with HP1 proteins: a link between the promyelocytic leukemia-associated nuclear bodies and the chromatin compartment. Proc. Natl. Acad. Sci. U. S. A. **95:**7316–7321. http://dx.doi.org/10.1073/pnas.95.13.7316.
19. **Burnett E, Christensen J, Tattersall P.** 2001. A consensus DNA recognition motif for two KDWK transcription factors identifies flexible-length, CpG-methylation sensitive cognate binding sites in the majority of human promoters. J. Mol. Biol. **314:**1029–1039. http://dx.doi.org/10.1006/jmbi.2000.5198.
20. **Newhart A, Negorev DG, Rafalska-Metcalf IU, Yang T, Maul GG, Janicki SM.** 2013. Sp100A promotes chromatin decondensation at a cytomegalovirus-promoter-regulated transcription site. Mol. Biol. Cell **24:**1454–1468. http://dx.doi.org/10.1091/mbc.E12-09-0669.
21. **Sternsdorf T, Jensen K, Will H.** 1997. Evidence for covalent modification of the nuclear dot-associated proteins PML and Sp100 by PIC1/SUMO-1. J. Cell Biol. **139:**1621–1634. http://dx.doi.org/10.1083/jcb.139.7.1621.
22. **Muller S, Matunis MJ, Dejean A.** 1998. Conjugation with the ubiquitin-related modifier SUMO-1 regulates the partitioning of PML within the nucleus. EMBO J. **17:**61–70. http://dx.doi.org/10.1093/emboj/17.1.61.
23. **Ascoli CA, Maul GG.** 1991. Identification of a novel nuclear domain. J. Cell Biol. **112:**785–795. http://dx.doi.org/10.1083/jcb.112.5.785.
24. **Chang KS, Stass SA, Chu DT, Deaven LL, Trujillo JM, Freireich EJ.** 1992. Characterization of a fusion cDNA (RARA/myl) transcribed from the t(15;17) translocation breakpoint in acute promyelocytic leukemia. Mol. Cell. Biol. **12:**800–810.
25. **Kakizuka A, Miller WH, Jr, Umesono K, Warrell RP, Jr, Frankel SR, Murty VV, Dmitrovsky E, Evans RM.** 1991. Chromosomal translocation t(15;17) in human acute promyelocytic leukemia fuses RAR alpha with a novel putative transcription factor, PML. Cell **66:**663–674. http://dx.doi.org/10.1016/0092-8674(91)90112-C.
26. **Dyck JA, Maul GG, Miller WH, Jr, Chen JD, Kakizuka A, Evans RM.** 1994. A novel macromolecular structure is a target of the promyelocyte-retinoic acid receptor oncoprotein. Cell **76:**333–343. http://dx.doi.org/10.1016/0092-8674(94)90340-9.
27. **de The H, Lavau C, Marchio A, Chomienne C, Degos L, Dejean A.** 1991. The PML-RAR alpha fusion mRNA generated by the t(15;17) translocation in acute promyelocytic leukemia encodes a functionally altered RAR. Cell **66:**675–684. http://dx.doi.org/10.1016/0092-8674(91)90113-D.
28. **Kastner P, Perez A, Lutz Y, Rochette-Egly C, Gaub MP, Durand B, Lanotte M, Berger R, Chambon P.** 1992. Structure, localization and transcriptional properties of two classes of retinoic acid receptor alpha fusion proteins in acute promyelocytic leukemia (APL): structural similarities with a new family of oncoproteins. EMBO J. **11:**629–642.
29. **Goddard AD, Borrow J, Solomon E.** 1992. A previously uncharacterized gene, PML, is fused to the retinoic acid receptor alpha gene in acute promyelocytic leukaemia. Leukemia **6**(Suppl 3)**:**117S–119S.
30. **Melnick A, Fruchtman S, Zelent A, Liu M, Huang Q, Boczkowska B, Calasanz M, Fernandez A, Licht JD, Najfeld V.** 1999. Identification of novel chromosomal rearrangements in acute myelogenous leukemia involving loci on chromosome 2p23, 15q22 and 17q21. Leukemia **13:**1534–1538.
31. **Melnick A, Licht JD.** 1999. Deconstructing a disease: RARalpha, its fusion partners, and their roles in the pathogenesis of acute promyelocytic leukemia. Blood **93:**3167–3215.
32. **Koken MH, Puvion-Dutilleul F, Guillemin MC, Viron A, Linares-Cruz G, Stuurman N, de Jong L, Szostecki C, Calvo F, Chomienne C.** 1994. The t(15;17) translocation alters a nuclear body in a retinoic acid-reversible fashion. EMBO J. **13:**1073–1083.

33. **Weis K, Rambaud S, Lavau C, Jansen J, Carvalho T, Carmo-Fonseca M, Lamond A, Dejean A.** 1994. Retinoic acid regulates aberrant nuclear localization of PML-RAR alpha in acute promyelocytic leukemia cells. Cell **76:**345–356. http://dx.doi.org/10.1016/0092-8674(94)90341-7.
34. **Sternsdorf T, Guldner HH, Szostecki C, Grotzinger T, Will H.** 1995. Two nuclear dot-associated proteins, PML and Sp100, are often co-autoimmunogenic in patients with primary biliary cirrhosis. Scand. J. Immunol. **42:**257–268. http://dx.doi.org/10.1111/j.1365-3083.1995.tb03652.x.
35. **Tavalai N, Stamminger T.** 2008. New insights into the role of the subnuclear structure ND10 for viral infection. Biochim. Biophys. Acta **1783:**2207–2221. http://dx.doi.org/10.1016/j.bbamcr.2008.08.004.
36. **Lavau C, Marchio A, Fagioli M, Jansen J, Falini B, Lebon P, Grosveld F, Pandolfi PP, Pelicci PG, Dejean A.** 1995. The acute promyelocytic leukaemia-associated PML gene is induced by interferon. Oncogene **11:**871–876.
37. **Everett RD, Chelbi-Alix MK.** 2007. PML and PML nuclear bodies: implications in antiviral defence. Biochimie **89:**819–830. http://dx.doi.org/10.1016/j.biochi.2007.01.004.
38. **Geoffroy MC, Chelbi-Alix MK.** 2011. Role of promyelocytic leukemia protein in host antiviral defense. J. Interferon Cytokine Res. **31:**145–158. http://dx.doi.org/10.1089/jir.2010.0111.
39. **Ishov AM, Sotnikov AG, Negorev D, Vladimirova OV, Neff N, Kamitani T, Yeh ET, Strauss JF, 3rd, Maul GG.** 1999. PML is critical for ND10 formation and recruits the PML-interacting protein daxx to this nuclear structure when modified by SUMO-1. J. Cell Biol. **147:**221–234. http://dx.doi.org/10.1083/jcb.147.2.221.
40. **Shen TH, Lin HK, Scaglioni PP, Yung TM, Pandolfi PP.** 2006. The mechanisms of PML-nuclear body formation. Mol. Cell **24:**331–339. http://dx.doi.org/10.1016/j.molcel.2006.09.013.
41. **Bernardi R, Pandolfi PP.** 2007. Structure, dynamics and functions of promyelocytic leukaemia nuclear bodies. Nat. Rev. Mol. Cell Biol. **8:**1006–1016. http://dx.doi.org/10.1038/nrm2277.
42. **Zhong S, Muller S, Ronchetti S, Freemont PS, Dejean A, Pandolfi PP.** 2000. Role of SUMO-1-modified PML in nuclear body formation. Blood **95:**2748–2752.
43. **Boddy MN, Howe K, Etkin LD, Solomon E, Freemont PS.** 1996. PIC 1, a novel ubiquitin-like protein which interacts with the PML component of a multiprotein complex that is disrupted in acute promyelocytic leukaemia. Oncogene **13:**971–982.
44. **Fu C, Ahmed K, Ding H, Ding X, Lan J, Yang Z, Miao Y, Zhu Y, Shi Y, Zhu J, Huang H, Yao X.** 2005. Stabilization of PML nuclear localization by conjugation and oligomerization of SUMO-3. Oncogene **24:**5401–5413. http://dx.doi.org/10.1038/sj.onc.1208714.
45. **Seeler JS, Dejean A.** 2003. Nuclear and unclear functions of SUMO. Nat. Rev. Mol. Cell Biol. **4:**690–699. http://dx.doi.org/10.1038/nrm1200.
46. **Lang M, Jegou T, Chung I, Richter K, Munch S, Udvarhelyi A, Cremer C, Hemmerich P, Engelhardt J, Hell SW, Rippe K.** 2010. Three-dimensional organization of promyelocytic leukemia nuclear bodies. J. Cell Sci. **123:**392–400. http://dx.doi.org/10.1242/jcs.053496.
47. **Hay RT.** 2005. SUMO: a history of modification. Mol. Cell **18:**1–12. http://dx.doi.org/10.1016/j.molcel.2005.03.012.
48. **Wimmer P, Schreiner S, Everett RD, Sirma H, Groitl P, Dobner T.** 2010. SUMO modification of E1B-55K oncoprotein regulates isoform-specific binding to the tumour suppressor protein PML. Oncogene **29:**5511–5522. http://dx.doi.org/10.1038/onc.2010.284.
49. **Wimmer P, Schreiner S, Dobner T.** 2012. Human pathogens and the host cell SUMOylation system. J. Virol. **86:**642–654. http://dx.doi.org/10.1128/JVI.06227-11.
50. **Wimmer P, Blanchette P, Schreiner S, Ching W, Groitl P, Berscheminski J, Branton PE, Will H, Dobner T.** 2013. Cross-talk between phosphorylation and SUMOylation regulates transforming activities of an adenoviral oncoprotein. Oncogene **32:**1626–1637. http://dx.doi.org/10.1038/onc.2012.187.
51. **Chelbi-Alix MK, Quignon F, Pelicano L, Koken MHM, de Thé H.** 1998. Resistance to virus infection conferred by the interferon-induced promyelocytic leukemia protein. J. Virol. **72:**1043–1051.
52. **Berscheminski J, Groitl P, Dobner T, Wimmer P, Schreiner S.** 2013. The adenoviral oncogene E1A-13S interacts with a specific isoform of the tumor suppressor PML to enhance viral transcription. J. Virol. **87:**965–977. http://dx.doi.org/10.1128/JVI.02023-12.
53. **Tatham MH, Rodriguez MS, Xirodimas DP, Hay RT.** 2009. Detection of protein SUMOylation in vivo. Nat. Protoc. **4:**1363–1371. http://dx.doi.org/10.1038/nprot.2009.128.
54. **Gripon P, Rumin S, Urban S, Le Seyec J, Glaise D, Cannie I, Guyomard C, Lucas J, Trepo C, Guguen-Guillouzo C.** 2002. Infection of a human hepatoma cell line by hepatitis B virus. Proc. Natl. Acad. Sci. U. S. A. **99:**15655–15660. http://dx.doi.org/10.1073/pnas.232137699.
55. **Everett RD, Parada C, Gripon P, Sirma H, Orr A.** 2008. Replication of ICP0-null mutant herpes simplex virus type 1 is restricted by both PML and Sp100. J. Virol. **82:**2661–2672. http://dx.doi.org/10.1128/JVI.02308-07.
56. **Mitsudomi T, Oyama T, Gazdar AF, Minna JD, Okabayashi K, Shirakusa T.** 1992. Mutations of ras and p53 genes in human non-small cell lung cancer cell lines and their clinical significance. Nihon Geka Gakkai Zasshi **93:**944–947.
57. **Schreiner S, Bürck C, Glass M, Groitl P, Wimmer P, Kinkley S, Mund A, Everett RD, Dobner T.** 2013. Control of human adenovirus type 5 (Ad5) gene expression by cellular Daxx/ATRX chromatin-associated complexes. Nucleic Acids Res. **41:**3532–3550. http://dx.doi.org/10.1093/nar/gkt064.
58. **Guldner HH, Szostecki C, Schroder P, Matschl U, Jensen K, Luders C, Will H, Sternsdorf T.** 1999. Splice variants of the nuclear dot-associated Sp100 protein contain homologies to HMG-1 and a human nuclear phosphoprotein-box motif. J. Cell Sci. **112:**733–747.
59. **Muller D, Schreiner S, Schmid M, Groitl P, Winkler M, Dobner T.** 2012. Functional cooperation between human adenovirus type 5 early region 4, open reading frame 6 protein, and cellular homeobox protein HoxB7. J. Virol. **86:**8296–8308. http://dx.doi.org/10.1128/JVI.00222-12.
60. **Groitl P, Dobner T.** 2007. Construction of adenovirus type 5 early region 1 and 4 virus mutants. Methods Mol. Med. **130:**29–39.
61. **Kindsmuller K, Schreiner S, Leinenkugel F, Groitl P, Kremmer E, Dobner T.** 2009. A 49-kilodalton isoform of the adenovirus type 5 early region 1B 55-kilodalton protein is sufficient to support virus replication. J. Virol. **83:**9045–9056. http://dx.doi.org/10.1128/JVI.00728-09.
62. **Forrester NA, Patel RN, Speiseder T, Groitl P, Sedgwick GG, Shimwell NJ, Seed RI, Catnaigh PO, McCabe CJ, Stewart GS, Dobner T, Grand RJ, Martin A, Turnell AS.** 2012. Adenovirus E4orf3 targets transcriptional intermediary factor 1gamma for proteasome-dependent degradation during infection. J. Virol. **86:**3167–3179. http://dx.doi.org/10.1128/JVI.06583-11.
63. **Schreiner S, Martinez R, Groitl P, Rayne F, Vaillant R, Wimmer P, Bossis G, Sternsdorf T, Ruszsics Z, Dobner T, Wodrich H.** 2012. Transcriptional activation of the adenoviral genome is mediated by capsid protein. PLoS Pathog. **8:**e1002549. http://dx.doi.org/10.1371/journal.ppat.1002549.
64. **Reich NC, Sarnow P, Duprey E, Levine AJ.** 1983. Monoclonal antibodies which recognize native and denatured forms of the adenovirus DNA-binding protein. Virology **128:**480–484. http://dx.doi.org/10.1016/0042-6822(83)90274-X.
65. **Sarnow P, Sullivan CA, Levine AJ.** 1982. A monoclonal antibody detecting the adenovirus type 5–E1b-58Kd tumor antigen: characterization of the E1b-58Kd tumor antigen in adenovirus-infected and -transformed cells. Virology **120:**510–517. http://dx.doi.org/10.1016/0042-6822(82)90054-X.
66. **Marton MJ, Baim SB, Ornelles DA, Shenk T.** 1990. The adenovirus E4 17-kilodalton protein complexes with the cellular transcription factor E2F, altering its DNA-binding properties and stimulating E1A-independent accumulation of E2 mRNA. J. Virol. **64:**2345–2359.
67. **Nevels M, Spruss T, Wolf H, Dobner T.** 1999. The adenovirus E4orf6 protein contributes to malignant transformation by antagonizing E1A-induced accumulation of the tumor suppressor protein p53. Oncogene **18:**9–17. http://dx.doi.org/10.1038/sj.onc.1202284.
68. **Kindsmuller K, Groitl P, Hartl B, Blanchette P, Hauber J, Dobner T.** 2007. Intranuclear targeting and nuclear export of the adenovirus E1B-55K protein are regulated by SUMO1 conjugation. Proc. Natl. Acad. Sci. U. S. A. **104:**6684–6689. http://dx.doi.org/10.1073/pnas.0702158104.
69. **Wimmer P, Blanchette P, Schreiner S, Ching W, Groitl P, Berscheminski J, Branton PE, Will H, Dobner T.** 2013. Cross-talk between phosphorylation and SUMOylation regulates transforming activities of an adenoviral oncoprotein. Oncogene **32:**1626–1637. http://dx.doi.org/10.1038/onc.2012.187.
70. **Endter C, Hartl B, Spruss T, Hauber J, Dobner T.** 2005. Blockage of CRM1-dependent nuclear export of the adenovirus type 5 early region

1B 55-kDa protein augments oncogenic transformation of primary rat cells. Oncogene **24:**55–64. http://dx.doi.org/10.1038/sj.onc.1208170.
71. **Rodriguez MS, Desterro JM, Lain S, Midgley CA, Lane DP, Hay RT.** 1999. SUMO-1 modification activates the transcriptional response of p53. EMBO J. **18:**6455–6461. http://dx.doi.org/10.1093/emboj/18.22.6455.
72. **Schreiner S, Wimmer P, Sirma H, Everett RD, Blanchette P, Groitl P, Dobner T.** 2010. Proteasome-dependent degradation of Daxx by the viral E1B-55K protein in human adenovirus-infected cells. J. Virol. **84:**7029–7038. http://dx.doi.org/10.1128/JVI.00074-10.
73. **Cuchet D, Sykes A, Nicolas A, Orr A, Murray J, Sirma H, Heeren J, Bartelt A, Everett RD.** 2011. PML isoforms I and II participate in PML-dependent restriction of HSV-1 replication. J. Cell Sci. **124:**280–291. http://dx.doi.org/10.1242/jcs.075390.
74. **Doucas V, Ishov AM, Romo A, Juguilon H, Weitzman MD, Evans RM, Maul GG.** 1996. Adenovirus replication is coupled with the dynamic properties of the PML nuclear structure. Genes Dev. **10:**196–207. http://dx.doi.org/10.1101/gad.10.2.196.
75. **Schreiner S, Kinkley S, Bürck C, Mund A, Wimmer P, Schubert T, Groitl P, Will H, Dobner T.** 2013. SPOC1-mediated antiviral host cell response is antagonized early in human adenovirus type 5 infection. PLoS Pathog. **9:**e1003775. http://dx.doi.org/10.1371/journal.ppat.1003775.
76. **Yousef AF, Fonseca GJ, Pelka P, Ablack JN, Walsh C, Dick FA, Bazett-Jones DP, Shaw GS, Mymryk JS.** 2010. Identification of a molecular recognition feature in the E1A oncoprotein that binds the SUMO conjugase UBC9 and likely interferes with polySUMOylation. Oncogene **29:**4693–4704. http://dx.doi.org/10.1038/onc.2010.226.
77. **Ledl A, Schmidt D, Muller S.** 2005. Viral oncoproteins E1A and E7 and cellular LxCxE proteins repress SUMO modification of the retinoblastoma tumor suppressor. Oncogene **24:**3810–3818. http://dx.doi.org/10.1038/sj.onc.1208539.
78. **Schreiner S, Burck C, Glass M, Groitl P, Wimmer P, Kinkley S, Mund A, Everett RD, Dobner T.** 2013. Control of human adenovirus type 5 gene expression by cellular Daxx/ATRX chromatin-associated complexes. Nucleic Acids Res. **41:**3532–3550. http://dx.doi.org/10.1093/nar/gkt064.
79. **Farr A, Roman A.** 1992. A pitfall of using a second plasmid to determine transfection efficiency. Nucleic Acids Res. **20:**920. http://dx.doi.org/10.1093/nar/20.4.920.
80. **Ibrahim NM, Marinovic AC, Price SR, Young LG, Frohlich O.** 2000. Pitfall of an internal control plasmid: response of Renilla luciferase (pRL-TK) plasmid to dihydrotestosterone and dexamethasone. Biotechniques **29:**782–784.
81. **Mulholland DJ, Cox M, Read J, Rennie P, Nelson C.** 2004. Androgen responsiveness of Renilla luciferase reporter vectors is promoter, transgene, and cell line dependent. Prostate **59:**115–119. http://dx.doi.org/10.1002/pros.20059.
82. **Vesuna F, Winnard P, Jr, Raman V.** 2005. Enhanced green fluorescent protein as an alternative control reporter to Renilla luciferase. Anal. Biochem. **342:**345–347. http://dx.doi.org/10.1016/j.ab.2005.04.047.
83. **Cuchet-Lourenco D, Boutell C, Lukashchuk V, Grant K, Sykes A, Murray J, Orr A, Everett RD.** 2011. SUMO pathway dependent recruitment of cellular repressors to herpes simplex virus type 1 genomes. PLoS Pathog. **7:**e1002123. http://dx.doi.org/10.1371/journal.ppat.1002123.
84. **Shenk T.** 2001. Adenoviridae: the viruses and their replication, p 2265–2300. *In* Knipe DM, Howley PM, Griffin DE, Lamb RA, Martin MA, Roizman B, Straus SE (ed), Fields virology, 4th ed. Lippincott Williams & Wilkins, Philadelphia, PA.
85. **Puvion-Dutilleul F, Chelbi-Alix MK, Koken M, Quignon F, Puvion E, de The H.** 1995. Adenovirus infection induces rearrangements in the intranuclear distribution of the nuclear body-associated PML protein. Exp. Cell Res. **218:**9–16. http://dx.doi.org/10.1006/excr.1995.1125.
86. **Hoppe A, Beech SJ, Dimmock J, Leppard KN.** 2006. Interaction of the adenovirus type 5 E4 Orf3 protein with promyelocytic leukemia protein isoform II is required for ND10 disruption. J. Virol. **80:**3042–3049. http://dx.doi.org/10.1128/JVI.80.6.3042-3049.2006.
87. **La Cour T, Gupta R, Rapacki K, Skriver K, Poulsen FM, Brunak S.** 2003. NESbase version 1.0: a database of nuclear export signals. Nucleic Acids Res. **31:**393–396. http://dx.doi.org/10.1093/nar/gkg101.
88. **Leppard KN, Emmott E, Cortese MS, Rich T.** 2009. Adenovirus type 5 E4 Orf3 protein targets promyelocytic leukaemia (PML) protein nuclear domains for disruption via a sequence in PML isoform II that is predicted as a protein interaction site by bioinformatic analysis. J. Gen. Virol. **90:**95–104. http://dx.doi.org/10.1099/vir.0.005512-0.
89. **Carvalho T, Seeler JS, Ohman K, Jordan P, Pettersson U, Akusjarvi G, Carmo-Fonseca M, Dejean A.** 1995. Targeting of adenovirus E1A and E4-ORF3 proteins to nuclear matrix-associated PML bodies. J. Cell Biol. **131:**45–56. http://dx.doi.org/10.1083/jcb.131.1.45.
90. **Leppard KN, Everett RD.** 1999. The adenovirus type 5 E1b 55K and E4 Orf3 proteins associate in infected cells and affect ND10 components. J. Gen. Virol. **80:**997–1008.
91. **Stracker TH, Lee DV, Carson CT, Araujo FD, Ornelles DA, Weitzman MD.** 2005. Serotype-specific reorganization of the Mre11 complex by adenoviral E4orf3 proteins. J. Virol. **79:**6664–6673. http://dx.doi.org/10.1128/JVI.79.11.6664-6673.2005.
92. **Everett RD.** 2001. DNA viruses and viral proteins that interact with PML nuclear bodies. Oncogene **20:**7266–7273. http://dx.doi.org/10.1038/sj.onc.1204759.
93. **Wimmer P, Schreiner S, Everett RD, Sirma H, Groitl P, Dobner T.** 2010. SUMO modification of E1B-55K oncoprotein regulates isoform-specific binding to the tumour suppressor protein PML. Oncogene **29:**5511–5522. http://dx.doi.org/10.1038/onc.2010.284.
94. **König C, Roth J, Dobbelstein M.** 1999. Adenovirus type 5 E4orf3 protein relieves p53 inhibition by E1B-55-kilodalton protein. J. Virol. **73:**2253–2262.
95. **Pennella MA, Liu Y, Woo JL, Kim CA, Berk AJ.** 2010. Adenovirus E1B 55-kilodalton protein is a p53-SUMO1 E3 ligase that represses p53 and stimulates its nuclear export through interactions with promyelocytic leukemia nuclear bodies. J. Virol. **84:**12210–12225. http://dx.doi.org/10.1128/JVI.01442-10.
96. **Muller S, Dobner T.** 2008. The adenovirus E1B-55K oncoprotein induces SUMO modification of p53. Cell Cycle **7:**754–758. http://dx.doi.org/10.4161/cc.7.6.5495.
97. **Lethbridge KJ, Scott GE, Leppard KN.** 2003. Nuclear matrix localization and SUMO-1 modification of adenovirus type 5 E1b 55K protein are controlled by E4 Orf6 protein. J. Gen. Virol. **84:**259–268. http://dx.doi.org/10.1099/vir.0.18820-0.
98. **Blanchette P, Cheng CY, Yan Q, Ketner G, Ornelles DA, Dobner T, Conaway RC, Conaway JW, Branton PE.** 2004. Both BC-box motifs of adenovirus protein E4orf6 are required to efficiently assemble an E3 ligase complex that degrades p53. Mol. Cell. Biol. **24:**9619–9629. http://dx.doi.org/10.1128/MCB.24.21.9619-9629.2004.
99. **Querido E, Blanchette P, Yan Q, Kamura T, Morrison M, Boivin D, Kaelin WG, Conaway RC, Conaway JW, Branton PE.** 2001. Degradation of p53 by adenovirus E4orf6 and E1B55K proteins occurs via a novel mechanism involving a Cullin-containing complex. Genes Dev. **15:**3104–3117. http://dx.doi.org/10.1101/gad.926401.
100. **Querido E, Marcellus RC, Lai A, Charbonneau R, Teodoro JG, Ketner G, Branton PE.** 1997. Regulation of p53 levels by the E1B 55-kilodalton protein and E4orf6 in adenovirus-infected cells. J. Virol. **71:**3788–3798.
101. **Sarnow P, Hearing P, Anderson CW, Halbert DN, Shenk T, Levine AJ.** 1984. Adenovirus early region 1B 58,000-dalton tumor antigen is physically associated with an early region 4 25,000-dalton protein in productively infected cells. J. Virol. **49:**692–700.
102. **Sarnow P, Ho YS, Williams J, Levine AJ.** 1982. Adenovirus E1b-58kd tumor antigen and SV40 large tumor antigen are physically associated with the same 54 kd cellular protein in transformed cells. Cell **28:**387–394. http://dx.doi.org/10.1016/0092-8674(82)90356-7.
103. **Maul GG, Everett RD.** 1994. The nuclear location of PML, a cellular member of the C3HC4 zinc-binding domain protein family, is rearranged during herpes simplex virus infection by the C3HC4 viral protein ICP0. J. Gen. Virol. **75:**1223–1233. http://dx.doi.org/10.1099/0022-1317-75-6-1223.
104. **Everett RD, Meredith M, Orr A, Cross A, Kathoria M, Parkinson J.** 1997. A novel ubiquitin-specific protease is dynamically associated with the PML nuclear domain and binds to a herpesvirus regulatory protein. EMBO J. **16:**1519–1530. http://dx.doi.org/10.1093/emboj/16.7.1519.
105. **Maul GG, Guldner HH, Spivack JG.** 1993. Modification of discrete nuclear domains induced by herpes simplex virus type 1 immediate early gene 1 product (ICP0). J. Gen. Virol. **74:**2679–2690. http://dx.doi.org/10.1099/0022-1317-74-12-2679.
106. **Burkham J, Coen DM, Hwang CB, Weller SK.** 2001. Interactions of herpes simplex virus type 1 with ND10 and recruitment of PML to replication compartments. J. Virol. **75:**2353–2367. http://dx.doi.org/10.1128/JVI.75.5.2353-2367.2001.
107. **Burkham J, Coen DM, Weller SK.** 1998. ND10 protein PML is recruited to herpes simplex virus type 1 prereplicative sites and replication com-

partments in the presence of viral DNA polymerase. J. Virol. **72:**10100–10107.
108. **Chelbi-Alix MK, de The H.** 1999. Herpes virus induced proteasome-dependent degradation of the nuclear bodies-associated PML and Sp100 proteins. Oncogene **18:**935–941. http://dx.doi.org/10.1038/sj.onc.1202366.
109. **Everett RD, Freemont P, Saitoh H, Dasso M, Orr A, Kathoria M, Parkinson J.** 1998. The disruption of ND10 during herpes simplex virus infection correlates with the Vmw110- and proteasome-dependent loss of several PML isoforms. J. Virol. **72:**6581–6591.
110. **Muller S, Dejean A.** 1999. Viral immediate-early proteins abrogate the modification by SUMO-1 of PML and Sp100 proteins, correlating with nuclear body disruption. J. Virol. **73:**5137–5143.
111. **Parkinson J, Everett RD.** 2000. Alphaherpesvirus proteins related to herpes simplex virus type 1 ICP0 affect cellular structures and proteins. J. Virol. **74:**10006–10017. http://dx.doi.org/10.1128/JVI.74.21.10006-10017.2000.
112. **Kim YE, Lee JH, Kim ET, Shin HJ, Gu SY, Seol HS, Ling PD, Lee CH, Ahn JH.** 2011. Human cytomegalovirus infection causes degradation of Sp100 proteins that suppress viral gene expression. J. Virol. **85:**11928–11937. http://dx.doi.org/10.1128/JVI.00758-11.
113. **Full F, Reuter N, Zielke K, Stamminger T, Ensser A.** 2012. Herpesvirus saimiri antagonizes nuclear domain 10-instituted intrinsic immunity via an ORF3-mediated selective degradation of cellular protein Sp100. J. Virol. **86:**3541–3553. http://dx.doi.org/10.1128/JVI.06992-11.
114. **Negorev DG, Vladimirova OV, Ivanov A, Rauscher F, 3rd, Maul GG.** 2006. Differential role of Sp100 isoforms in interferon-mediated repression of herpes simplex virus type 1 immediate-early protein expression. J. Virol. **80:**8019–8029. http://dx.doi.org/10.1128/JVI.02164-05.
115. **Turnell AS, Grand RJ.** 2012. DNA viruses and the cellular DNA-damage response. J. Gen. Virol. **93:**2076–2097. http://dx.doi.org/10.1099/vir.0.044412-0.
116. **Tavalai N, Adler M, Scherer M, Riedl Y, Stamminger T.** 2011. Evidence for a dual antiviral role of the major nuclear domain 10 component Sp100 during the immediate-early and late phases of the human cytomegalovirus replication cycle. J. Virol. **85:**9447–9458. http://dx.doi.org/10.1128/JVI.00870-11.
117. **Dinant C, Luijsterburg MS.** 2009. The emerging role of HP1 in the DNA damage response. Mol. Cell. Biol. **29:**6335–6340. http://dx.doi.org/10.1128/MCB.01048-09.
118. **Baldeyron C, Soria G, Roche D, Cook AJ, Almouzni G.** 2011. HP1alpha recruitment to DNA damage by p150CAF-1 promotes homologous recombination repair. J. Cell Biol. **193:**81–95. http://dx.doi.org/10.1083/jcb.201101030.
119. **Ling PD, Peng RS, Nakajima A, Yu JH, Tan J, Moses SM, Yang WH, Zhao B, Kieff E, Bloch KD, Bloch DB.** 2005. Mediation of Epstein-Barr virus EBNA-LP transcriptional coactivation by Sp100. EMBO J. **24:**3565–3575. http://dx.doi.org/10.1038/sj.emboj.7600820.